Spectrally stable encapsulated vortices for nonlinear Schrödinger equations

R. L. Pego* and H. A. Warchall†

June 2001 (revised January 2002)

Abstract

A large class of multidimensional nonlinear Schrödinger equations admit localized nonradial standing wave solutions that carry nonzero intrinsic angular momentum. Here we provide evidence that certain of these spinning excitations are spectrally stable. We find such waves for equations in two space dimensions with *focusing-defocusing* nonlinearities, such as cubic-quintic. Spectrally stable waves resemble a vortex (non-localized solution with asymptotically constant amplitude) cut off at large radius by a kink layer that exponentially localizes the solution.

For the evolution equations linearized about a localized spinning wave, we prove that unstable eigenvalues are zeros of Evans functions for a finite set of ordinary differential equations. Numerical computations indicate that there exist spectrally stable standing waves having central vortex of any degree.

Key Words: solitary wave, stability, instability, multidimensional solitons, vortices, Evans function, saturable media, vortex soliton, azimuthal modes, polydiacetylene para-toluene sulfonate

AMS Classifications: 35Q55, 35B55, 34B40, 35P15, 35Q51, 78A60

Running head: Stability of encapsulated vortices

1 Introduction

A long-term goal of the study of nonlinear waves is to sort out what kinds of structures and interactions are significant and robust. From this point of view, nonlinear Schrödinger equations are worthy of study because of their status as a canonical model for weakly nonlinear phenomena in many fields (including nonlinear optics as a prominent example), and as a simple model for more complicated gauge theories of mathematical physics. In more than one space dimension such equations admit a variety of solutions with interesting structure, including solitary waves (e.g., "light bullets") and vortices (kin to the magnetic vortices of the theory of superconductivity).

Here we consider nonlinear Schrödinger equations of the form

$$-i\,\partial_t u - \Delta u = g(u) \tag{1.1}$$

where $u\colon \mathbb{R}^{2+1} \to \mathbb{C}$, and where $g(u) = h(|u|^2)u$ for some real-valued C^1 function h. Our most significant results concern nonlinearities for which focusing ($h' > 0$) at small amplitude is overcome by defocusing ($h' < 0$) at larger amplitude. Prototypical is the cubic-quintic nonlinearity

$$g(u) = |u|^2 u - |u|^4 u. \tag{1.2}$$

*Department of Mathematics & Institute for Physical Science and Technology, University of Maryland, College Park MD 20742

†Department of Mathematics, University of North Texas, Denton TX 76203 and Division of Mathematical Sciences, National Science Foundation

Much of the theory developed in this paper also applies to equations of focusing type.

We are interested in the stability of solitary-wave solutions with the symmetry of a vortex, having the special form

$$u_0(x,t) = e^{i\omega t + im\theta} w(r) \tag{1.3}$$

in terms of polar coordinates (r,θ) for $\mathbb{R}^2$. Here ω is a real constant (the standing wave frequency), m is an integer (the vortex degree), and $w\colon [0,\infty) \to \mathbb{R}$. We also refer to m as the spin of the wave, because the conserved quantity L that corresponds via Noether's principle to the rotational invariance of (1.1) is the (third component of the) angular momentum

$$\int_{\mathbb{R}^2} (-ix \times \nabla u)\overline{u}.$$

For standing waves having the form (1.3), $L = 2\pi m \int_0^\infty w^2 r\, dr$.

The standing-wave amplitude profile w in (1.3) must satisfy the differential equation

$$w'' + \frac{1}{r}w' - \frac{m^2}{r^2}w + f(w) = 0, \tag{1.4}$$

where $f(w) = g(w) - \omega w$. It is known that, under suitable conditions on f, for each integer m this equation has C^2 solutions w such that $w(r) \to 0$ exponentially as $r \to \infty$. Iaia and Warchall [15] proved that for fixed m, there is at least one such solution w for each prescribed number n of positive zeros. Each such solution gives rise to a localized standing wave solution of (1.1). In turn, this gives rise to solitary-wave solutions traveling at any speed, via the Galilean boost transformation for the Schrödinger equation.

Without loss of generality we assume $h(0) = 0$. Then the restriction of g to the real axis is a C^1 function with $g'(0) = 0$ and $g'(s) = O(s^2)$ as $s \to 0$. For an exponentially localized solution to exist, it is necessary that $f'(0) < 0$, so the standing-wave frequency ω is positive. It is also necessary that $F(s) \equiv \int_0^s f(\sigma)\, d\sigma$ be positive for some positive value of s attained by profile amplitudes $w(r)$.

In this paper we investigate the linear stability of such exponentially localized solitary waves. Linearizing (1.1) about such a solution yields a real system of the form $\partial_t \Phi = A\Phi$ where A is a 2×2 matrix of second-order partial differential operators that has purely imaginary essential spectrum $\sigma_{\text{ess}} = \{i\tau : |\tau| \geq \omega\}$. Any eigenvalues of A not in the essential spectrum are discrete (isolated and of finite multiplicity) and occur with Hamiltonian symmetry: If λ is an eigenvalue, then so are $-\lambda$ and $\overline{\lambda}$.

We prove that the search for unstable eigenvalues of A reduces to the study of a finite number of eigenvalue problems for 2×2 systems of second-order ordinary differential equations. Eigenvalues for each of these systems correspond to zeros of an Evans function or Wronskian that we prove is a globally analytic function in the cut plane $\mathbb{C}_\sigma = \mathbb{C} \setminus \sigma_{\text{ess}}$. The real part of any unstable eigenvalue is bounded by a quantity determined from the profile shape.

We use the argument principle and numerical computation to locate zeros of the Evans functions. Very often the operator A has unstable eigenvalues (meaning eigenvalues with positive real part), indicating that the associated solitary wave is linearly exponentially unstable with respect to perturbations of initial data.

However, we have discovered spectrally stable waves (waves with no unstable eigenvalues) in a certain parameter regime for several nonlinearities of focusing-defocusing type, including the cubic-quintic (1.2). All of these waves have radial profiles $w(r)$ with no positive zeros. We have found such waves for all values of spin index satisfying $|m| \leq 5$, with indications that they exist for arbitrary m.

The spectrally stable spinning waves ($m \neq 0$) are found when ω is close to but less than a critical value ω_* for which the two bounded regions between the graphs of $y = g(x)$ and $y = \omega_* x$ for $x \geq 0$ have *equal area*. This condition on ω_* is equivalent to the condition that the potential function F with $\omega = \omega_*$ has a zero-height local maximum or "hilltop" at a point $a_* > 0$. For the cubic-quintic

case $\omega_* = \frac{3}{16} = 0.1875$ and spectrally stable waves are found for ω in an interval $\omega_{\rm cr}(m) < \omega < \omega_*$ which shrinks as $|m|$ increases, with width roughly proportional to $|m|^{-2}$.

A transition to instability occurs as the standing wave frequency ω decreases below $\omega_{\rm cr}$. Unstable eigenvalues appear, for a particular azimuthal mode, due to collisions of pairs of imaginary eigenvalues as in a Hamiltonian Hopf bifurcation.

The waves develop a distinctive structure as ω approaches ω_* from below. (See Figs. 5 and 6 in section 2.) The wave amplitude $w(r)$ increases from zero to remain approximately constant over a large r-interval, taking values near a_*, near the hilltop of the nonlinear potential F, before rapidly returning exponentially to zero. Thus the waves have a structure consisting of a core region resembling a *vortex* (a non-localized solution with asymptotically constant amplitude, cf. [22]), encapsulated or cut off (at an apparently arbitrarily large radius) by a circular *kink* region that serves to exponentially localize the solution.

What are the salient features of the nonlinearity that might explain the existence of stable encapsulated vortices with this kind of structure? We believe that a basic understanding begins with the stability of spatially constant solutions

$$u(x,t) = ae^{i\omega t} \tag{1.5}$$

where $a > 0$ is constant and $\omega = g(a)/a$. This solution is linearly unstable if $h'(a^2) > 0$ (the focusing case) and is linearly stable if $h'(a^2) < 0$ (defocusing); see [23] and Remark 3.2 below. Equivalently, stability is determined by the sign of $g'(a) - g(a)/a$, a quantity that is easily visualized on the graph of g over the positive reals. The spatially constant solution $ae^{i\omega t}$ is linearly unstable if $g'(a) - g(a)/a > 0$ and linearly stable if $g'(a) - g(a)/a < 0$.

A focusing-defocusing nonlinearity like the cubic-quintic (1.2) has two features that appear to be key (see Fig. 1):

(i) There is a number $a_0 > 0$ such that the constant-state solution (1.5) is linearly unstable for $0 < a < a_0$ ($h'(a^2) > 0$) and is linearly stable for $a > a_0$ ($h'(a^2) < 0$).

(ii) There is a number $\omega_* > 0$ for which the graphs of $y = g(x)$ and $y = \omega_* x$ enclose two regions of equal area, and so for which the potential F has zero-height hilltops at $s = 0$ and at $s = a_* > 0$.

As we discuss in section 6, for any nonlinearity with these properties there is a linearly stable one-dimensional kink solution of (1.1) that connects the state $a_* e^{i\omega_* t}$ to the zero state. The value ω_* is the standing-wave frequency of the kink. In the limit as ω approaches ω_* and $|m| \to \infty$, we will see that the structure of the encapsulated vortices consists of parts that approximate linearly stable solutions (constant states or kinks). In this way it becomes plausible that these waves are linearly stable.

The nonlinear Schrödinger equation is of fundamental importance in nonlinear optics, where a cubic (Kerr) nonlinearity is most often assumed. A substantial body of work exists on so-called saturable media, for which the nonlinearity takes the form

$$g(u) = \frac{|u|^2 u}{1 + |u|^2}. \tag{1.6}$$

The cubic-quintic nonlinearity (1.2) can be obtained by truncating the Taylor expansion for this nonlinearity, but in fact there is a substantial difference between the saturable and cubic-quintic nonlinearities at large amplitude. This difference is reflected in the stability of spinning solitary waves. In the saturable case the spinning waves with $|m| = 1$ have been found to be unstable [12]. Some spinning waves with $|m| = 1$ for the cubic-quintic nonlinearity (1.2), however, have previously been found to be stable in direct numerical simulations by Quiroga-Teixeiro and Michinel [27]. We conjecture that the crucial difference is that the cubic-quintic is focusing-defocusing, but the saturable nonlinearity is only focusing — it does not admit any linearly stable nonzero constant states.

There is experimental evidence that the cubic-quintic model is in fact appropriate for certain optical materials [18, 17, 19, 11]. Instabilities of three-dimensional spinning waves for the cubic-quintic model have been investigated numerically in [9, 21, 20]. After this paper was first submitted, we learned of work of Towers *et al.* on the two-dimensional cubic-quintic model [31]. These authors numerically obtain stability results essentially similar to ours, with one discrepancy concerning the existence of a very weak instability for a range of values of ω in cases for $|m| = 1, 2, 3$ where we find stability. For related work on solitary waves with vortex symmetry in nonlinear Ginzburg-Landau equations and quadratically nonlinear optical media, see [8, 30].

The cubic-quintic nonlinear Schrödinger equation can also been considered a nonrelativistic version of a simple model in nuclear physics that admits nontopological solitons called "Q-balls" [6]. The results of this paper may be relevant to the issue of the stability of closed cylindrical Q-walls raised in [5].

For radially symmetric waves ($m = 0$), an energy-based criterion for instability was established by Shatah and Strauss [28] and a stability criterion was established by Grillakis, Shatah and Strauss [13]. The result is that waves in a family parametrized by ω are stable if $dN/d\omega > 0$ and are unstable if $dN/d\omega < 0$, where $N = \int_{\mathbb{R}^2} |u_0|^2$. Consistent with previous studies [4, 10, 35] we find that all spinless waves for the cubic-quintic (1.2) are stable, but if the sign of the quintic term is reversed then all waves become unstable. Our numerical results elucidate the mechanism of the transition to instability as the coefficient of the quintic term changes sign continuously. A single pair of imaginary eigenvalues collides at the origin and a pair of real eigenvalues emerge with opposite sign. A related scenario occurs for solitary waves of generalized Korteweg-de Vries equations [26] in which unstable eigenvalues emerge at the origin (out of the continuous spectrum) as the sign of $dN/d\omega$ changes, and suggests that stability criteria based on the sign of $dN/d\omega$ will not detect instability transitions that are not associated with eigenvalues moving through the origin.

For the spinning solitary waves of the nonlinear Schrödinger equation under consideration ($m \neq 0$), it is not known whether spectral stability is mathematically a sufficient condition for nonlinear stability (modulo symmetries of the wave family as appropriate). It is conceivable that instability could be created by nonlinear resonance phenomena involving both localized oscillatory modes and radiation modes in the continuous spectrum, such as have been studied by Soffer and Weinstein [29]. If these waves ultimately turn out to be unstable, however, the absence of unstable eigenvalues suggests that they would enjoy a long "lifetime" under perturbation, and that any instability mechanism would be a subtle one.

This paper is organized as follows. In section 2, we survey the structure of solitary wave solutions to (1.1) as the standing-wave frequency, spin, and node number vary, contrasting the cubic-quintic nonlinearity (1.2) with a pure cubic. We linearize about a solitary wave and prove some fundamental results concerning the spectrum of the operator A in section 3. In particular, in section 3.2 we establish that we can locate all unstable eigenvalues of A by analyzing a finite number of ordinary differential equations. In section 4 we introduce and analyze the Evans functions and Wronskians associated with the eigenvalue problem. A representation of the Evans function in terms of exterior products, described by Alexander and Sachs [3], proves to be convenient for purposes both theoretical and numerical. We present numerical results in section 5. In section 6 we discuss heuristic reasons why encapsulated-vortex solutions may become stable in a limiting parameter regime.

2 Taxonomy of solitary waves with spin

In this section we illustrate the structure of the solitary-wave profiles $w(r)$ for various choices of spin m, node number n and standing wave frequency ω, contrasting two different types of nonlinearity for which existence proofs of infinite families of localized standing waves have been given [14, 15, 16]. In particular we contrast the cubic-quintic nonlinearity in (1.2) with the pure cubic

$$g(u) = |u|^2 u. \tag{2.1}$$

Because of the invariance of (1.1) under spatial reflection, we may assume that $m \geq 0$.

Localized solutions of equation (1.4) for standing wave profiles have the asymptotic behavior (see [14])

$$w(r) \sim \begin{cases} d_0 r^m & \text{as } r \to 0^+, \\ \dfrac{d_\infty e^{-\sigma r}}{\sqrt{r}} & \text{as } r \to \infty, \end{cases} \tag{2.2}$$

for some constants d_0 and d_∞, where $\sigma = \sqrt{-f'(0)} = \sqrt{\omega} > 0$. More precisely, where its amplitude is small the behavior of $w(r)$ is governed by the linear equation

$$w'' + \frac{1}{r}w' - \frac{m^2}{r^2}w - \sigma^2 w = 0. \tag{2.3}$$

Linearly independent solutions of this equation are the modified Bessel functions $I_m(\sigma r)$ and $K_m(\sigma r)$, which have the asymptotic behavior

$$\begin{aligned} I_m(\sigma r) &\sim \frac{1}{2^m m!}(\sigma r)^m, \qquad & K_m(\sigma r) &\sim 2^{m-1}(m-1)!\,(\sigma r)^{-m}, \qquad & (r \to 0^+) \\ I_m(\sigma r) &\sim \frac{1}{\sqrt{2\pi\sigma r}}\, e^{\sigma r}, \qquad & K_m(\sigma r) &\sim \sqrt{\frac{\pi}{2\sigma r}}\, e^{-\sigma r} & (r \to \infty) \end{aligned} \tag{2.4}$$

except in the case $m = 0$, when $K_0(\sigma r) \sim -\ln r$ as $r \to 0^+$.

We compute solutions to equation (1.4) numerically by a shooting method, based on small-amplitude approximations of the form $w(r) \sim \tilde{d}_0 I_m(\sigma r)$ for small r ($m > 0$), $w(r) \sim \tilde{d}_\infty K_m(\sigma r)$ for large r. For a suitably small initial radius r_0, we numerically solve the initial-value problem for (1.4) with initial data $w(r_0) = \tilde{d}_0 I_m(\sigma r_0)$ and $w'(r_0) = \tilde{d}_0 \sigma I'_m(\sigma r_0)$. We vary the parameter $\tilde{d}_0$ (equivalently d_0) so that at some large radius r_1, the solution and its derivative are small and assume the proper asymptotic form, satisfying $w'(r_1)/w(r_1) = \sigma K'_m(\sigma r_1)/K_m(\sigma r_1)$.

In Fig. 2 we plot the potential F for the cubic and cubic-quintic nonlinearities, taking $\omega = 1$ and $\omega = .175$ respectively. We may interpret (1.4) as an equation of motion for a point with position $w(r)$ at time r moving in the potential well $F(w) - \frac{1}{2}m^2 w^2/r^2$, subject to the time-dependent damping force $-w'/r$. As $r \to \infty$, the particle "balances" on top of the hill at $w = 0$. Nodes in the radial profile occur when the particle crosses the top of this hill. Since the hilltop at the origin is an unstable equilibrium of this one-dimensional "motion," solutions satisfying $w(r) \to 0$ as $r \to \infty$ are found for $\tilde{d}_0$ in a discrete set.

Cubic. In the case of a cubic nonlinearity $g(u) = \gamma|u|^2 u$ with $\gamma > 0$, we may always scale so that $\gamma = 1$ and $\omega = 1$, by replacing $w(r)$ by $\sqrt{\omega/\gamma}\,\tilde{w}(\sqrt{\omega}r)$. Figure 3 shows the nodeless ($n = 0$) wave profiles for spin values $m = 0$, 1, 3 and 6.

The form of the nodeless waves varies with m in a way that can be understood as follows. It appears that as m becomes large, $w(r)$ remains small initially on a large interval, and then is approximated near its maximum at $r = R$ by $\phi_a(r - R)$, where ϕ_a is the even positive localized solution on $(-\infty, \infty)$ of

$$\phi'' - a^2\phi + \phi^3 = 0. \tag{2.5}$$

with $a = \sqrt{1 + (m/R)^2}$. Explicitly, $\phi_a(x) = \sqrt{2}\,a\,\mathrm{sech}^2\, ax$. We will argue in appendix A that $R \approx \sqrt{2}m$, so that $\max \phi_a(x) = \sqrt{3}$. This approximation agrees well with the numerical solution shown in Fig. 3.

Cubic-quintic. In the case of a cubic-quintic nonlinearity $g(u) = \gamma|u|^2 u - \delta|u|^4 u$ with positive constants γ and δ, we can scale so there is one free parameter $\omega > 0$, and $\gamma = \delta = 1$. The condition that $F(w) > 0$ for some w is then equivalent to the requirement that

$$\omega < \omega_* \equiv \frac{3}{16} = 0.1875. \tag{2.6}$$

When this holds, $F(w)$ achieves its maximum value at a point $w = w_{\max} > 0$ which depends on ω. Potentials F with this additional local maximum are called hilltop potentials in [15] and [16]. We write $F_{\max} = F(w_{\max})$ and note that $w_{\max}^2 = \frac{1}{2} + \frac{1}{2}\sqrt{1-4\omega}$. For $\omega = \omega_*$ we get $w_{\max} = a_* \equiv \sqrt{3}/2$. Figure 4 shows nodeless profiles with $\omega = 0.18$ for spin values $m = 0$, 1, 2, 3.

We demonstrate the effect of varying ω in Figures 5 and 6, where we plot nodeless profiles for spins $m = 1$ and 3, respectively. As ω approaches ω_* from below, the height $F_{\max}$ of the rightmost hilltop in the graph of F decreases to zero, and the "particle" at position $w(r)$ spends more "time" near $w_{\max}$, resulting in flatter profiles. This is the phenomenon of "loitering at the hilltop" studied in [15] and [16], also see [6]. It is precisely in this "flattop" regime that we find nodeless waves with no unstable eigenvalues for any m, as discussed in Section 5.

The wave profiles develop a structure in this regime that can be described more precisely. It is shown in [15] that for any $\omega \in (0, \omega_*)$, with an appropriate amplitude d in (2.2) one obtains a nonlocalized solution of (1.4) that increases monotonically to $w_{\max}$ as $r \to \infty$. This yields a vortex solution to (1.1). Note that for ω near ω_*, the profiles in Figures 5 and 6 resemble a vortex profile cut off by a kink. Near the kink location at $r = R$ (where $w(r)$ last equals $\frac{1}{2}w_{\max}$, say), the profile is approximated by $\phi_*(r - R)$, where ϕ_* is the solution on $(-\infty, \infty)$ of

$$\phi'' + g(\phi) - \omega_* w = 0 \tag{2.7}$$

that satisfies

$$\phi_*(r) \to a_* \text{ as } r \to -\infty, \quad \phi_*(r) \to 0 \text{ as } r \to \infty, \quad \phi_*(0) = \frac{1}{2}a_*. \tag{2.8}$$

We note that a one-dimensional kink solution of (1.1) of the form $u(x, y, t) = e^{i\omega_* t}\phi_*(x)$ exists for any nonlinearity with $h \in C^1$ that has the properties (i) and (ii) stated in the introduction.

Fig. 4 suggests also that as the spin m increases, the wave structure contains a flipped inner kink that also moves out away from the origin. We formally analyze the asymptotic behavior of the kink locations as $\omega \to \omega_*$ in appendix A.

3 Linearization and reduction to ordinary differential equations

In this section we linearize (1.1) about a given exponentially localized solution of the form (1.3) and prove a number of fundamental results that concern the associated spectrum and eigenvalues. In particular, we prove in Theorem 3.4 that the search for unstable eigenvalues reduces to the study of a finite number of eigenvalue problems for 2×2 systems of second-order ordinary differential equations.

We consider a solution $u(x, t)$ to (1.1) that results from a perturbation to the initial condition $u_0(x, 0) = v_0(x)$ for a standing wave solution $u_0(x, t) = e^{i\omega t}v_0(x)$ where $v_0(x) = e^{im\theta}w(r)$ with $w(r) \to 0$ exponentially as $r \to \infty$. We write

$$u(x, t) = e^{i\omega t}\left(v_0(x) + v(x, t)\right) \tag{3.1}$$

and linearize the nonlinear terms in the evolution equation for the perturbation v around amplitude $v = 0$. We compute that

$$g(v_0 + v) - g(v_0) = \alpha(w)v + \beta(w)e^{2im\theta}\bar{v} + O(|v|^2) \tag{3.2}$$

where

$$\alpha(s) = \frac{1}{2}\left[g'(s) + \frac{1}{s}g(s)\right], \quad \beta(s) = \frac{1}{2}\left[g'(s) - \frac{1}{s}g(s)\right] \tag{3.3}$$

for $s \neq 0$, with $\alpha(0) = \beta(0) = 0$. Here g' refers to the ordinary derivative of the real-valued restriction of g to real arguments. Note that because g is not holomorphic, its linearization is not

complex-linear but only real-linear. Also note that $g'(s) = O(s^2)$, so $\alpha(s) = O(s^2)$ and $\beta(s) = O(s^2)$ as $s \to 0$.

Thus the linearized evolution equation for the perturbation v may be written

$$-i\,\partial_t v = \Delta v - \sigma^2 v + \alpha(w)v + \beta(w)e^{2im\theta}\bar{v} \tag{3.4}$$

where $\sigma^2 = \omega > 0$. We next represent the linearized evolution equation as a pair of real equations for the components of

$$\Phi \equiv \begin{pmatrix} \Phi_1 \\ \Phi_2 \end{pmatrix} \equiv \begin{pmatrix} \mathrm{Re}\, v \\ \mathrm{Im}\, v \end{pmatrix} \in \mathbb{R}^2, \tag{3.5}$$

so that $v = \Phi_1 + i\Phi_2$. Setting

$$J \equiv \begin{pmatrix} 0 & -1 \\ 1 & 0 \end{pmatrix}, \quad R \equiv \begin{pmatrix} 1 & 0 \\ 0 & -1 \end{pmatrix}, \tag{3.6}$$

we rewrite equation (3.4) as

$$\partial_t \Phi = A\Phi \equiv J\left(\Delta - \sigma^2 + \alpha(w(r)) + \beta(w(r))e^{2m\theta J}R\right)\Phi. \tag{3.7}$$

3.1 Spectrum and eigenvalues

As a first step toward understanding the stability properties of the standing waves, we investigate the spectrum of A, regarded as an unbounded operator on the space $L^2(\mathbb{R}^2, \mathbb{R}^2)$ of square-integrable functions with values in $\mathbb{R}^2$. The domain of A is the Sobolev space $H^2(\mathbb{R}^2, \mathbb{R}^2)$ of functions into $\mathbb{R}^2$ whose derivatives up to order 2 are square-integrable. This space is complexified to study the spectrum of A, which we denote by $\sigma(A)$. The spectrum of A consists of two parts, the discrete spectrum $\sigma_{\mathrm{disc}}(A)$, consisting of isolated eigenvalues of finite multiplicity, and the essential spectrum $\sigma_{\mathrm{ess}}(A)$, which consists of everything else and is determined by the "operator at infinity" defined by

$$A_0 = J(\Delta - \sigma^2).$$

Lemma 3.1 *The spectrum of A is the union of the discrete and essential spectrum. The latter is purely imaginary and is given by*

$$\sigma_{\mathrm{ess}}(A) = \sigma(A_0) = \{it \mid t \in \mathbb{R} \text{ and } |t| \geq \sigma^2\}.$$

Proof The spectrum of A_0 is easily determined using the Fourier transform. It consists of the set of all eigenvalues of the matrix $J(-\xi^2 - \sigma^2)$ as ξ varies over $\mathbb{R}$. This set is equal to $\{it \mid t \in \mathbb{R} \text{ and } |t| \geq \sigma^2\}$.

The operator $A - A_0$ is a multiplier with coefficients that are continuous and bounded and decay exponentially as $r \to \infty$. Consequently, it is easy to show (using the convenient compactness criterion of [25], for example) that A is a relatively compact perturbation of A_0, meaning that for $\lambda \notin \sigma(A_0)$ the operator $(\lambda - A_0)^{-1}(A - A_0)$ is compact. From Weyl's theorem, it follows that A and A_0 have the same essential spectrum. □

Remark 3.2 We briefly digress to consider the linearization of (1.1) about the spatially constant solution $u_0(t) = ae^{i\omega t}$. One may assume $a > 0$ without loss of generality, and one has $\omega = g(a)/a$ and $\alpha(a) - \omega = \beta(a) = a^2 h'(a^2)$. Linearization yields the constant-coefficient operator $A_a = J(\Delta + \beta(a) + \beta(a)R)$, whose spectrum is the set $\{\pm\lambda(\xi) \mid \xi \in \mathbb{R}^2\}$ where $\lambda(\xi) = i\sqrt{(|\xi|^2 - \beta(a))^2 - \beta(a)^2}$,

which is purely imaginary if and only if $\beta(a) \leq 0$. Hence the solution $ae^{i\omega t}$ is spectrally stable if and only if $h'(|a|^2) \leq 0$.

By Lemma 3.1, our primary concern becomes the discrete spectrum of A in (3.7). We will search for eigenfunctions Ψ of A taking values in $\mathbb{C}^2$. The operator A has real coefficients and has the special form $A = JL$ where L is self-adjoint. Consequently eigenvalues occur with Hamiltonian symmetry: If λ is an eigenvalue with eigenfunction Ψ, then $\bar{\lambda}$ and $-\lambda$ are eigenvalues. This is because $\bar{\Psi}$ is also an eigenfunction of A with eigenvalue $\bar{\lambda}$, and $J\Psi$ is an eigenfunction of the adjoint $A^* = -LJ$ with eigenvalue $-\lambda$. Note that if λ is complex with nonzero imaginary part, then the real and imaginary parts of $e^{\lambda t}\Psi$ are *real* solutions to the differential equation (3.7) that are linearly independent.

The equation $A\Psi = \lambda\Psi$ is equivalent to

$$(\lambda J - \sigma^2 + \Delta + \alpha)\Psi + \beta e^{2m\theta J} R\Psi = 0. \tag{3.8}$$

Suppose Ψ is a square-integrable solution of (3.8). We represent $\Psi(r,\theta) \in \mathbb{C}^2$ via eigenvectors of J:

$$\Psi = \psi_+ \begin{pmatrix} 1/2 \\ -i/2 \end{pmatrix} + \psi_- \begin{pmatrix} 1/2 \\ i/2 \end{pmatrix}, \tag{3.9}$$

where $\psi_+(r,\theta)$ and $\psi_-(r,\theta)$ are complex-valued. Since

$$J\Psi = i\psi_+ \begin{pmatrix} 1/2 \\ -i/2 \end{pmatrix} - i\psi_- \begin{pmatrix} 1/2 \\ i/2 \end{pmatrix}, \quad R\Psi = \psi_- \begin{pmatrix} 1/2 \\ -i/2 \end{pmatrix} + \psi_+ \begin{pmatrix} 1/2 \\ i/2 \end{pmatrix}, \tag{3.10}$$

taking the components of 3.8 gives

$$\begin{array}{rcl} (i\lambda - \sigma^2 + \Delta + \alpha)\psi_+ + \beta e^{2im\theta}\psi_- & = & 0, \\ (-i\lambda - \sigma^2 + \Delta + \alpha)\psi_- + \beta e^{-2im\theta}\psi_+ & = & 0. \end{array} \tag{3.11}$$

Since ψ_+ and ψ_- are square-integrable and $\alpha(w(r))$, $\beta(w(r))$ are bounded, it follows that ψ_+, ψ_- lie in the Sobolev space $H^2(\mathbb{R}^2)$. In particular, they are Hölder-continuous functions.

We next expand ψ_+ and ψ_- in Fourier series with respect to θ:

$$\psi_\pm(r,\theta) = \sum_{n=-\infty}^{\infty} e^{in\theta} y_\pm^{(n)}(r), \tag{3.12}$$

with

$$y_\pm^{(n)}(r) = \frac{1}{2\pi}\int_0^{2\pi} \psi_\pm(r,\theta) e^{-in\theta}\, d\theta. \tag{3.13}$$

This is an orthogonal expansion and each term lies in $H^2(\mathbb{R}^2)$. It will prove notationally convenient to shift the summation index and write instead

$$\psi_\pm(r,\theta) = \sum_{j=-\infty}^{\infty} e^{i(j\pm m)\theta} y_\pm^{(j\pm m)}(r). \tag{3.14}$$

The Fourier coefficients then satisfy

$$\begin{array}{rcl} (i\lambda - \sigma^2 + \Delta_r - r^{-2}(j+m)^2 + \alpha) y_+^{(j+m)} + \beta y_-^{(j-m)} & = & 0, \\ (-i\lambda - \sigma^2 + \Delta_r - r^{-2}(j-m)^2 + \alpha) y_-^{(j-m)} + \beta y_+^{(j+m)} & = & 0, \end{array} \tag{3.15}$$

and satisfy the boundary conditions

$$\lim_{r\to 0^+} y_\pm^{(j\pm m)}(r) \text{ exists}, \quad \text{and} \quad \lim_{r\to\infty} y_\pm^{(j\pm m)}(r) = 0. \tag{3.16}$$

Here $\Delta_r \equiv \frac{\partial^2}{\partial r^2} + \frac{1}{r}\frac{\partial}{\partial r}$ is the radial Laplacian.

For each integer value of j, equations (3.15) are a system of second-order ordinary differential equations for the two functions $y_+^{(j+m)}(r)$ and $y_-^{(j-m)}(r)$. There is no coupling between these systems for different values of j. Summarizing, we have proved the "only if" part of the following:

Proposition 3.3 *A complex number $\lambda \notin \sigma_{\rm ess}(A)$ is an eigenvalue of A in L^2 if and only if for some integer j, equations (3.15) have a nontrivial solution satisfying (3.16).*

To prove the "if" part, we claim that if there are nontrivial solutions $y_\pm^{(j\pm m,\lambda)}$ to equations (3.15)–(3.16) for some λ and some j, then

$$\Psi^{(j,\lambda)} = \begin{pmatrix} 1/2 \\ -i/2 \end{pmatrix} e^{i(j+m)\theta} y_+^{(j+m,\lambda)}(r) + \begin{pmatrix} 1/2 \\ i/2 \end{pmatrix} e^{i(j-m)\theta} y_-^{(j-m,\lambda)}(r) \tag{3.17}$$

is an eigenvector of A with eigenvalue λ. Clearly $\Psi = \Psi^{(j,\lambda)}$ satisfies (3.8) except perhaps at the origin. We must show that $\Psi \in H^2(\mathbb{R}^2, \mathbb{R}^2)$. It follows from (2.2) and the theory of asymptotic behavior of ODEs (see [7] and Subsection 4.1 below) that solutions of (3.15) that decay to zero as $r \to \infty$ must decay at an exponential rate, together with their derivatives. Therefore $\Psi \in L^2(\mathbb{R}^2, \mathbb{R}^2)$. Furthermore, solutions that approach a limit as $r \to 0$ must have bounded derivatives. It follows that Ψ satisfies (3.8) in the sense of distributions, and from this it follows that $\Psi \in H^2(\mathbb{R}^2, \mathbb{R}^2)$. This proves the Proposition. □

Corresponding to the complex eigenvector (3.17) of the operator A are the two real-valued solutions

$$\Phi_{(a)}^{(j,\lambda)}(t) \equiv \mathrm{Re}\,(e^{\lambda t}\Psi^{(j,\lambda)}), \quad \Phi_{(b)}^{(j,\lambda)}(t) \equiv \mathrm{Im}\,(e^{\lambda t}\Psi^{(j,\lambda)}) \tag{3.18}$$

of the vector evolution equations (3.7), from which we recover two complex-valued solutions of the original linearized equation (3.4) via

$$v^{(a)}(t) = \Phi_{(a)1}^{(j,\lambda)}(t) + i\Phi_{(a)2}^{(j,\lambda)}(t), \quad v^{(b)}(t) = \Phi_{(b)1}^{(j,\lambda)}(t) + i\Phi_{(b)2}^{(j,\lambda)}(t). \tag{3.19}$$

Explicitly, we have:

$$\begin{aligned} v^{(a)}(t) &= \tfrac{1}{2}\left(e^{\lambda t}e^{i(j+m)\theta}y_+ + \overline{e^{\lambda t}e^{i(j-m)\theta}y_-}\right), \\ v^{(b)}(t) &= \tfrac{1}{2i}\left(e^{\lambda t}e^{i(j+m)\theta}y_+ - \overline{e^{\lambda t}e^{i(j-m)\theta}y_-}\right). \end{aligned} \tag{3.20}$$

Since any real linear combination of $v_{(a)}$ and $v_{(b)}$ is also a solution, the general solution to the linearized equation (3.4) corresponding to eigenvalue λ and index j is

$$v(x,t) = \left(ce^{\lambda t}e^{i(j+m)\theta}y_+^{(j+m,\lambda)}(r) + \overline{ce^{\lambda t}e^{i(j-m)\theta}y_-^{(j-m,\lambda)}(r)}\right) \tag{3.21}$$

where c is any complex constant. If we were to take the time-zero value of this function $v(x,0)$ as a perturbation to the initial conditions $v_0(x)$ for (1.1), we would expect the nonlinear time evolution of v to be well-approximated by (3.21) for small time.

We note that j measures the departure of the perturbation v from the angular dependence of u_0. We will refer to j as the "twist" index.

3.2 Bounds on index for unstable eigenvalues

We have shown eigenvalues of the operator A correspond to eigenvalues of (3.15)-(3.16) for some value of the index j. To locate eigenvalues of the operator A, we use numerical techniques to locate eigenvalues of (3.15)–(3.16). This procedure at first appears intractable because there is a countably infinite set of equations to analyze. Our main result in this section, however, establishes that any eigenvalue with nonzero real part occurs in a system (3.15) with twist j in a finite set determined by the wave profile w alone.

Theorem 3.4 *Suppose that* $\operatorname{Re}\lambda \neq 0$*, where* λ *is an eigenvalue of* A *corresponding to a solution of (3.15)–(3.16) for some integer* j*. Then*

$$|j| \le j_{\max} := |m| + \sqrt{C_2}, \quad \textit{where} \quad C_2 = \max_{r\ge 0} r^2 \left(\alpha(w(r)) + |\beta(w(r))|\right).$$

Proof Let $\mu(s) = \alpha(s) + |\beta(s)|$. Then $\mu(0) = 0$ and $\mu(s) = \sigma^2 + \max\{f'(s), f(s)/s\}$ for $s \neq 0$. Because f is continuously differentiable, μ is continuous on $\mathbb{R}$, and we note that $\mu(r)$ takes on positive values because $f(w(r))$ does (otherwise the primitive $F(w(r))$ would never get positive). Because $\mu(s) = O(s)$ as $s \to 0$ and $w(r)$ is exponentially decaying at ∞, the maximum C_2 of $r^2\mu(w(r))$ is achieved, and we have $0 < C_2 < \infty$.

We note that with $y_\pm = y_\pm^{(j\pm m)}$, (3.15) can be written

$$L_j \mathbf{y} = \lambda K \mathbf{y}, \tag{3.22}$$

where

$$\mathbf{y} = \begin{pmatrix} y_+ \\ y_- \end{pmatrix}, \quad K = \begin{pmatrix} i & 0 \\ 0 & -i \end{pmatrix}, \tag{3.23}$$

and

$$L_j = \begin{pmatrix} \sigma^2 - \Delta_r + r^{-2}(j+m)^2 - \alpha & -\beta \\ -\beta & \sigma^2 - \Delta_r + r^{-2}(j-m)^2 - \alpha \end{pmatrix}. \tag{3.24}$$

Define inner products in $L^2(\mathbb{R}^+; r\,dr)$ and $L^2(\mathbb{R}^+, \mathbb{R}^2; r\,dr)$ by

$$\langle y, z\rangle = \int_0^\infty y(r)\overline{z(r)}\, r\, dr, \quad \langle \mathbf{y}|\mathbf{z}\rangle = \langle y_+, z_+\rangle + \langle y_-, z_-\rangle.$$

We claim that if $C_* := \min\{(j-m)^2, (j+m)^2\} > C_2$ and (3.22) has a nontrivial solution, then $\langle L_j\mathbf{y}|\mathbf{y}\rangle > 0$. To see this, recall that for a solution of (3.15)–(3.16), $y_\pm$ and its derivative are bounded as $r \to 0$ and decay exponentially as $r \to \infty$. We then have that $\left\langle (\sigma^2 - \Delta_r) y_\pm, y_\pm \right\rangle \ge 0$, therefore

$$\begin{aligned} \langle L_j\mathbf{y}|\mathbf{y}\rangle &\ge \int_0^\infty \left\{ \left(\frac{j+m}{r}\right)^2 |y_+|^2 + \left(\frac{j-m}{r}\right)^2 |y_-|^2 \right\} r\, dr \\ &\quad - \int_0^\infty \Big\{ \alpha\left(|y_+|^2 + |y_-|^2\right) + \beta\left(y_+\bar{y}_- + \bar{y}_+ y_-\right) \Big\} r\, dr \\ &\ge \int_0^\infty (C_* - C_2)\left(|y_+|^2 + |y_-|^2\right) r^{-1}\, dr > 0, \end{aligned}$$

where we used the facts that $\bar{y}z + y\bar{z} \le |y|^2 + |z|^2$ and $\alpha + |\beta| \le C_2/r^2$.

Now take the inner product of (3.22) with $\mathbf{y}$. Since $C_* = (|j| - |m|)^2$, if $|j| > |m| + \sqrt{C_2}$ we get

$$0 < \langle L_j\mathbf{y}|\mathbf{y}\rangle = \lambda \langle K\mathbf{y}|\mathbf{y}\rangle.$$

Since K is skew-adjoint, $\langle K\mathbf{y}|\mathbf{y}\rangle$ is purely imaginary, therefore λ must be purely imaginary. □

3.3 Bounds on eigenvalues

We show here that eigenvalues of A are confined to a vertical strip determined by the wave amplitude profile w.

Proposition 3.5 *If* λ *is an eigenvalue of* A*, then*

$$|\operatorname{Re}\lambda| \le \Lambda_{\max} := \max_{r\ge 0}\Big(|\alpha(w(r))| + |\beta(w(r))|\Big).$$

Proof Let $\tilde{A} = A - A_0 = J(\alpha + \beta e^{2m\theta J} R)$. Since the ℓ^2 matrix norms $|J|$, $|R|$ and $|e^{2m\theta J}|$ all equal 1, we have $|\tilde{A}| \le C_0 := \max_{r\ge 0}(|\alpha(w(r))| + |\beta(w(r))|)$. Note that $\lambda - A_0$ is the Fourier multiplier $\mathcal{F}(M)$ defined via $(\mathcal{F}(M)\Psi)\hat{}\,(\xi) = M(\xi)\hat{\Psi}(\xi)$, where

$$M(\xi) = \begin{pmatrix} \lambda & -\sigma^2 - |\xi|^2 \\ \sigma^2 + |\xi|^2 & \lambda \end{pmatrix}. \tag{3.25}$$

Suppose Ψ is an eigenfunction of A corresponding to an eigenvalue λ with nonzero real part. Then $0 = (\lambda - A_0 - \tilde{A})\Psi$, and $\lambda - A_0 = \mathcal{F}(M)$ is invertible, so that we have

$$(I - \mathcal{F}(M^{-1})\tilde{A})\Psi = 0. \tag{3.26}$$

Let $\mathcal{P}_\pm = \lambda \pm i(\sigma^2 + |\xi|^2)$. Then $\lambda = \frac{1}{2}(\mathcal{P}_+ + \mathcal{P}_-)$, $\sigma^2 + |\xi|^2 = \frac{1}{2i}(\mathcal{P}_+ - \mathcal{P}_-)$, so

$$M(\xi) = Q\,\mathrm{diag}\{\mathcal{P}_-, \mathcal{P}_+\}Q^{-1}, \qquad Q = \frac{1}{\sqrt{2}}\begin{pmatrix} 1 & 1 \\ i & -i \end{pmatrix}.$$

Note that Q is unitary and $M(\xi)^{-1} = Q\,\mathrm{diag}\{\mathcal{P}_-^{-1}, \mathcal{P}_+^{-1}\}Q^{-1}$, so the matrix norm $|M(\xi)^{-1}| \le \max|\mathcal{P}_\pm^{-1}| \le 1/|\operatorname{Re}\lambda|$. Therefore, the operator norm of $\mathcal{F}(M^{-1})\tilde{A}$ on L^2 is bounded by $C_0/|\operatorname{Re}\lambda|$. If $|\operatorname{Re}\lambda| > C_0$, then, there is no nontrivial solution of (3.26) in L^2. □

3.4 Symmetries

The value $\lambda = 0$ is always an eigenvalue of the operator A, with multiplicity greater than one, due to various symmetries of the original nonlinear Schrödinger equation (1.1) (e.g., translation, rotation, phase change). These symmetries and associated generalized eigenfunctions are described in detail in Appendix B.

The eigenvalue equations (3.15) also have simple symmetries connected to the Hamiltonian symmetry of A. From (3.15) and the orthogonal expansion in (3.14) it is easy to check the following.

Lemma 3.6 *Suppose (y_+, y_-) form a solution to (3.15) for some pair (λ, j). Then (y_-, y_+) form a solution for $(-\lambda, -j)$ and $(\bar{y}_-, \bar{y}_+)$ form a solution for $(\bar{\lambda}, -j)$. If λ is a real eigenvalue of A corresponding to index $j \neq 0$, then λ is (at least) a double eigenvalue.*

4 Detecting eigenvalues with Evans functions

In this section we prove that eigenvalues of the operator A of index j correspond to zeros of a certain analytic function $E_j(\lambda)$, which we call an Evans function for the system (3.15). This characterization of eigenvalues as zeros of an analytic function allows us to use the argument principle to count the total number of eigenvalues inside various contours in the complex plane.

We shall provide three equivalent expressions for this Evans function, in terms of a Wronskian, an adjoint system, and an associated exterior system. The last expression is used to establish the global analyticity of $E_j(\lambda)$ and is advantageous for reasons of numerical stability.

We develop the theory in this section only for the case of spinning waves for which $m \neq 0$. The spinless case $m = 0$ is different in several ways, primarily due to the nonzero value of the wave profile $w(r)$ at $r = 0$. For brevity's sake we omit any theoretical treatment of the spinless case, though in section 5 we report results of numerical computations performed for this case.

4.1 Asymptotic behavior of eigenfunctions.

Here we study the asymptotic behavior of solutions to (3.15) as $r \to 0^+$ and as $r \to \infty$. We fix the integer $m \neq 0$, the base wave radial profile w, the index j, and a complex number λ in the cut plane $\mathbb{C}_\sigma = \mathbb{C} \setminus \{i\tau : |\tau| \ge \sigma^2\}$.

Because $w(r) \to 0$ exponentially as $r \to \infty$, for large values of r the coefficients $\alpha(w(r))$ and $\beta(w(r))$ in (3.15) vanish exponentially quickly as $r \to \infty$. We thus expect that solutions to (3.15) will behave for large r like solutions of the decoupled equations

$$(i\lambda - \sigma^2 + \Delta_r - r^{-2}(j+m)^2)y_+ = 0, \tag{4.1}$$

$$(-i\lambda - \sigma^2 + \Delta_r - r^{-2}(j-m)^2)y_- = 0. \tag{4.2}$$

Solutions of (4.1) are linear combinations of the modified Bessel functions $I_{|j+m|}(k_+r)$ and $K_{|j+m|}(k_+r)$, and solutions of (4.2) are linear combinations of the modified Bessel functions $I_{|j-m|}(k_-r)$ and $K_{|j-m|}(k_-r)$, where

$$k_+ = \sqrt{\sigma^2 - i\lambda}, \quad k_- = \sqrt{\sigma^2 + i\lambda}, \tag{4.3}$$

with the principal branch of the square root taken. For brevity we write

$$\begin{array}{ll} I_+(r) = I_{|j+m|}(k_+r), & I_-(r) = I_{|j-m|}(k_-r), \\ K_+(r) = K_{|j+m|}(k_+r), & K_-(r) = K_{|j-m|}(k_-r). \end{array} \tag{4.4}$$

Since λ is in the cut plane, the complex numbers $k_\pm$ have positive real parts, and thus $|I_\pm(r)| \to \infty$ and $|K_\pm(r)| \to 0$ as $r \to \infty$.

Similarly, because $w(r) \to 0$ as $r \to 0^+$ when $m \geq 1$, we expect that solutions to (3.15) will also behave in this case like solutions of the decoupled equations (4.1), (4.2) for r near zero. Note that $|I_\pm(r)|$ is bounded and $|K_\pm(r)| \to \infty$ as $r \to 0$.

To make these observations precise, we reformulate (3.15) as a first-order system. We set

$$c_+(r) = k_+^2 + \left(\frac{j+m}{r}\right)^2, \quad c_-(r) = k_-^2 + \left(\frac{j-m}{r}\right)^2. \tag{4.5}$$

Then (3.15) is equivalent to the system

$$\boldsymbol{y}' = \boldsymbol{B}(r, j, \lambda)\boldsymbol{y} \tag{4.6}$$

with $\boldsymbol{B}(r, j, \lambda) = \mathring{\boldsymbol{B}}(r, j, \lambda) + \tilde{\boldsymbol{B}}(r)$, where, writing $y_+ = y_+^{(j+m)}$, $y_- = y_-^{(j-m)}$, we have

$$\boldsymbol{y} = \begin{pmatrix} y_+ \\ {y_+}' \\ y_- \\ {y_-}' \end{pmatrix}, \quad \mathring{\boldsymbol{B}} = \begin{pmatrix} 0 & 1 & 0 & 0 \\ c_+ & -1/r & 0 & 0 \\ 0 & 0 & 0 & 1 \\ 0 & 0 & c_- & -1/r \end{pmatrix}, \quad \tilde{\boldsymbol{B}} = \begin{pmatrix} 0 & 0 & 0 & 0 \\ -\alpha & 0 & -\beta & 0 \\ 0 & 0 & 0 & 0 \\ -\beta & 0 & -\alpha & 0 \end{pmatrix}. \tag{4.7}$$

Let $\mathring{\boldsymbol{y}}_i$, $i = 1, \ldots, 4$, denote the linearly independent solutions of the asymptotic system

$$\boldsymbol{y}' = \mathring{\boldsymbol{B}}(r, j, \lambda)\boldsymbol{y} \tag{4.8}$$

that form the columns of the fundamental matrix

$$\mathring{\boldsymbol{Y}} = \begin{pmatrix} I_+(r) & 0 & K_+(r) & 0 \\ I_+'(r) & 0 & K_+'(r) & 0 \\ 0 & I_-(r) & 0 & K_-(r) \\ 0 & I_-'(r) & 0 & K_-'(r) \end{pmatrix}. \tag{4.9}$$

Lemma 4.1 *Fix λ in the cut plane $\mathbb{C}_\sigma = \mathbb{C} \setminus \{i\tau : |\tau| \geq \sigma^2\}$, and let $m > 0$. Then there exist solutions $\boldsymbol{y}_i^{(0)}$ and $\boldsymbol{y}_i^{(\infty)}$ to the coupled system (4.6) such that*

$$\boldsymbol{y}_i^{(0)}(r) \sim \mathring{\boldsymbol{y}}_i(r) \quad \textit{as} \quad r \to 0^+, \tag{4.10}$$

$$\boldsymbol{y}_i^{(\infty)}(r) \sim \mathring{\boldsymbol{y}}_i(r) \quad \textit{as} \quad r \to \infty, \tag{4.11}$$

for $i = 1, 2, 3, 4$.

The proof of Lemma 4.1 is in Appendix C.1.

4.2 Evans function test for eigenvalues

We fix the spin $m \geq 1$, base wave w, index j, and a complex number λ in the cut plane $\mathbb{C}_\sigma$. To determine whether λ is an eigenvalue corresponding to index j, we wish to determine whether (3.15) has a nontrivial solution satisfying (3.16). This is equivalent to determining whether (4.6) has a bounded solution that vanishes as $r \to \infty$.

Let $\boldsymbol{y}_i^{(0)}$ and $\boldsymbol{y}_i^{(\infty)}$, $i = 1, \ldots, 4$, be solutions of (4.6) with the properties specified in Lemma 4.1. From Lemma 4.1 we know that the subspace S_0 of solutions $\boldsymbol{y}$ to (4.6) that are bounded as $r \to 0^+$ is spanned by $\boldsymbol{y}_1^{(0)}$ and $\boldsymbol{y}_2^{(0)}$. Also we know that the subspace S_∞ of solutions $\boldsymbol{y}$ to (4.6) that approach zero as $r \to \infty$ is spanned by $\boldsymbol{y}_3^{(\infty)}$ and $\boldsymbol{y}_4^{(\infty)}$.

The question of whether there are nontrivial solutions of (3.15) satisfying (3.16) for the value of λ under consideration is thus reduced to the question of whether the subspaces S_0 and S_∞ have nontrivial intersection. To answer this question, we may compute the Wronskian of the four solutions $\boldsymbol{y}_1^{(0)}$, $\boldsymbol{y}_2^{(0)}$, $\boldsymbol{y}_3^{(\infty)}$ and $\boldsymbol{y}_4^{(\infty)}$. Since there is a nontrivial intersection of S_0 and S_∞ if and only if these four vectors are linearly dependent, the Wronskian of these four vectors vanishes (identically in r) if and only if the number λ is an eigenvalue corresponding to index j.

We note that, since $\mathrm{tr}(\boldsymbol{B}) = -2/r$, by Abel's formula the quantity

$$E_j(\lambda) := -r^2 \det\left(\boldsymbol{y}_1^{(0)}, \boldsymbol{y}_2^{(0)}, \boldsymbol{y}_3^{(\infty)}, \boldsymbol{y}_4^{(\infty)}\right) \tag{4.12}$$

is independent of r. This normalized Wronskian is called the *Evans function* [2] associated with the system (4.6). Thus we have the following.

Proposition 4.2 *A complex number λ in the cut plane $\mathbb{C}_\sigma$ is an eigenvalue of A if and only if $E_j(\lambda) = 0$ for some integer j.*

We conclude this subsection by describing some symmetries of this Evans function.

Proposition 4.3 *For all integers j and complex numbers $\lambda \in \mathbb{C}_\sigma$,*

(i) $\overline{E_j(\lambda)} = E_j(-\overline{\lambda})$

(ii) $E_j(\lambda)$ *is real if* λ *is purely imaginary.*

(iii) $E_j(\lambda) = E_{-j}(-\lambda)$

Proof (i) Since taking the complex conjugate of (4.6) yields a solution of the same equation with λ replaced by $-\overline{\lambda}$, we find from (4.12) that $\overline{E_j(\lambda)} = E_j(-\overline{\lambda})$.

(ii) follows from (i), since $\lambda = -\overline{\lambda}$ if λ is purely imaginary.

(iii) We make use of the symmetry of equations (3.15) as described in subsection 3.4. If $\boldsymbol{y}$ is a solution of (4.6), then exchanging the first two components with the last two yields a solution of $\boldsymbol{y}' = \boldsymbol{B}(r, -j, -\lambda)\boldsymbol{y}$. Consequently, $E_{-j}(-\lambda)$ is obtained from $E_j(\lambda)$ in (4.12) by exchanging the first two rows with the last two. This leaves the determinant invariant, and then (iii) follows. □

4.3 The adjoint system

To obtain alternative characterizations of the Evans function, we consider next the adjoint system associated with (4.6),

$$\boldsymbol{z}' = -\boldsymbol{z}\boldsymbol{B}(r, j, \lambda). \tag{4.13}$$

Here $\boldsymbol{z}(r)$ is considered to be a row vector. Any solutions of (4.13) and (4.6) have the property that the product $\boldsymbol{z}(r) \cdot \boldsymbol{y}(r)$ is independent of r. The asymptotic adjoint system

$$\boldsymbol{z}' = -\boldsymbol{z}\,\mathring{\boldsymbol{B}}(r, j, \lambda) \tag{4.14}$$

has the fundamental set of solutions $\overset{\circ}{\boldsymbol{z}}_k$, $k = 1, \ldots, 4$ given by the rows of the matrix

$$\overset{\circ}{\boldsymbol{Z}}(r) = r \begin{pmatrix} -K'_+(r) & K_+(r) & 0 & 0 \\ 0 & 0 & -K'_-(r) & K_-(r) \\ I'_+(r) & -I_+(r) & 0 & 0 \\ 0 & 0 & I'_-(r) & -I_-(r) \end{pmatrix} \tag{4.15}$$

This matrix is the inverse of $\overset{\circ}{\boldsymbol{Y}}(r)$, i.e., we have $\overset{\circ}{\boldsymbol{Z}}\overset{\circ}{\boldsymbol{Y}} = I$.

Lemma 4.4 *The adjoint system (4.13) has solutions $\boldsymbol{z}_k^{(\infty)}$, $k = 1, \ldots, 4$ that satisfy*

$$\boldsymbol{z}_k^{(\infty)}(r) \sim \overset{\circ}{\boldsymbol{z}}_k(r) \quad \text{as } r \to \infty.$$

This lemma is proved in the same manner as Lemma 4.1, so we omit the details.

Let $\boldsymbol{z}_k^{(\infty)}$, $k = 1, \ldots, 4$, be solutions with the properties specified in Lemma 4.4. Let $Z^{(\infty)}(r)$ denote the matrix whose rows are $\boldsymbol{z}_k^{(\infty)}(r)$, and let $Y^{(\infty)}(r)$ be the matrix with columns $\boldsymbol{y}_k^{(\infty)}(r)$. Because of the limiting behavior as $r \to \infty$ expressed in Lemmas 4.1 and 4.4 and the fact that $\overset{\circ}{\boldsymbol{Z}}\overset{\circ}{\boldsymbol{Y}} = I$, it follows directly that

$$Z^{(\infty)}(r)Y^{(\infty)}(r) = I \tag{4.16}$$

for all $r > 0$; that is, $\boldsymbol{z}_k^{(\infty)}(r) \cdot \boldsymbol{y}_l^{(\infty)}(r) = \delta_{kl}$.

The matrix $Y^{(\infty)}$ is a fundamental matrix for the system (4.6). Therefore the solutions $\boldsymbol{y}_i^{(0)}$ of Lemma 4.1 admit representations of the form

$$\boldsymbol{y}_i^{(0)} = \sum_{k=1}^{4} \boldsymbol{y}_k^{(\infty)} \alpha_{ki} \tag{4.17}$$

with constant coefficients that are given by

$$\alpha_{ki} = \boldsymbol{z}_k^{(\infty)} \cdot \boldsymbol{y}_i^{(0)}.$$

The value λ is an eigenvalue of (3.15)–(3.16) if and only if the span of $\boldsymbol{y}_1^{(0)}$ and $\boldsymbol{y}_2^{(0)}$ nontrivially intersects the span of $\boldsymbol{y}_3^{(\infty)}$ and $\boldsymbol{y}_4^{(\infty)}$. This is equivalent to the statement that

$$\det \begin{pmatrix} \alpha_{11} & \alpha_{12} \\ \alpha_{21} & \alpha_{22} \end{pmatrix} = \det \begin{pmatrix} \boldsymbol{z}_1^{(\infty)} \cdot \boldsymbol{y}_1^{(0)} & \boldsymbol{z}_1^{(\infty)} \cdot \boldsymbol{y}_2^{(0)} \\ \boldsymbol{z}_2^{(\infty)} \cdot \boldsymbol{y}_1^{(0)} & \boldsymbol{z}_2^{(\infty)} \cdot \boldsymbol{y}_2^{(0)} \end{pmatrix} = 0. \tag{4.18}$$

It turns out that this determinant simply yields an alternative characterization of the Evans function.

Proposition 4.5 *For all integers j and complex numbers $\lambda \in \mathbb{C}_\sigma$,*

$$E_j(\lambda) = \det \begin{pmatrix} \boldsymbol{z}_1^{(\infty)} \cdot \boldsymbol{y}_1^{(0)} & \boldsymbol{z}_1^{(\infty)} \cdot \boldsymbol{y}_2^{(0)} \\ \boldsymbol{z}_2^{(\infty)} \cdot \boldsymbol{y}_1^{(0)} & \boldsymbol{z}_2^{(\infty)} \cdot \boldsymbol{y}_2^{(0)} \end{pmatrix}.$$

Proof

$$\begin{aligned} E_j(\lambda) &= -r^2 \det\left(\boldsymbol{y}_1^{(0)}, \boldsymbol{y}_2^{(0)}, \boldsymbol{y}_3^{(\infty)}, \boldsymbol{y}_4^{(\infty)}\right) \\ &= -r^2 \sum_{i,k=1}^{4} \alpha_{i1}\alpha_{k2} \det\left(\boldsymbol{y}_i^{(\infty)}, \boldsymbol{y}_k^{(\infty)}, \boldsymbol{y}_3^{(\infty)}, \boldsymbol{y}_4^{(\infty)}\right) \\ &= -r^2 \left(\alpha_{11}\alpha_{22} - \alpha_{21}\alpha_{12}\right) \det\left(\boldsymbol{y}_1^{(\infty)}, \boldsymbol{y}_2^{(\infty)}, \boldsymbol{y}_3^{(\infty)}, \boldsymbol{y}_4^{(\infty)}\right) \\ &= -r^2 \det\left(\boldsymbol{Y}^{(\infty)}\right) \left(\alpha_{11}\alpha_{22} - \alpha_{21}\alpha_{12}\right) \\ &= -r^2 \det\left(\boldsymbol{Y}^{(0)}\right) \left(\alpha_{11}\alpha_{22} - \alpha_{21}\alpha_{12}\right) \\ &= \det \begin{pmatrix} \boldsymbol{z}_1^{(\infty)} \cdot \boldsymbol{y}_1^{(0)} & \boldsymbol{z}_1^{(\infty)} \cdot \boldsymbol{y}_2^{(0)} \\ \boldsymbol{z}_2^{(\infty)} \cdot \boldsymbol{y}_1^{(0)} & \boldsymbol{z}_2^{(\infty)} \cdot \boldsymbol{y}_2^{(0)} \end{pmatrix}. \end{aligned}$$

Here we have used the fact that the r-independent quantities $r^2 \det\left(\boldsymbol{Y}^{(\infty)}\right)$ and $r^2 \det\left(\boldsymbol{Y}^{(0)}\right) = -1$ are equal by virtue of (4.11). □

4.4 Exterior systems and analyticity

According to our results so far, for each fixed λ in $\mathbb{C}_\sigma$, $E_j(\lambda)$ depends upon a choice of certain solutions $\boldsymbol{y}_i^{(0)}$ and $\boldsymbol{y}_i^{(\infty)}$ or $\boldsymbol{z}_i^{(\infty)}$ having the properties described in Lemmas 4.1 and 4.4. In this section, we establish that the value of $E_j(\lambda)$ is *independent* of this choice, and that E_j is an analytic function in the cut plane $\mathbb{C}_\sigma$.

The method of proof of Lemmas 4.1 and 4.4 could be used to establish that the required solutions can be chosen to depend analytically on λ, locally in the set $\mathbb{C}_\sigma$ in the complex plane. However, this approach does not guarantee that there is a single globally analytic choice, leaving the difficulty that a given set of choices may yield an Evans function that is not analytic in all of $\mathbb{C}_\sigma$.

This difficulty is obviated with an algebraic device described by Alexander and Sachs [3] (used by one of the present authors for numerical calculations mentioned in that paper) and recently employed by Afendikov and Bridges [1]. A similar device (called the compound matrix shooting method) has been used in numerical computations for boundary-value problems related to hydrodynamic stability theory [24].

One considers *exterior products* of solutions of the system (4.6) and the associated adjoint system (4.13). In the present context it suffices to consider exterior products of two solutions at a time.

In general, suppose $\boldsymbol{y}$ and $\tilde{\boldsymbol{y}}$ are vectors in $\mathbb{C}^n$ that, with respect to the standard basis vectors $\boldsymbol{e}_j$, $j = 1, \ldots, n$, have the expansions

$$\boldsymbol{y} = \sum_{j=1}^{n} y_j \boldsymbol{e}_j, \quad \tilde{\boldsymbol{y}} = \sum_{j=1}^{n} \tilde{y}_j \boldsymbol{e}_j. \tag{4.19}$$

Let $N = \binom{n}{2} = n(n-1)/2$ and let $\boldsymbol{y} \wedge \tilde{\boldsymbol{y}}$ denote the vector in $\mathbb{C}^N$ with components

$$(\boldsymbol{y} \wedge \tilde{\boldsymbol{y}})_{j \wedge k} = y_j \tilde{y}_k - y_k \tilde{y}_j = \det \begin{pmatrix} y_j & \tilde{y}_j \\ y_k & \tilde{y}_k \end{pmatrix} \tag{4.20}$$

for $j < k$. The vector $\boldsymbol{y} \wedge \tilde{\boldsymbol{y}} = -\tilde{\boldsymbol{y}} \wedge \boldsymbol{y}$ is called the exterior product of $\boldsymbol{y}$ and $\tilde{\boldsymbol{y}}$. For convenience, when $n = 4$ we order the components according to the identification

$$(1 \wedge 2,\ 1 \wedge 3,\ 1 \wedge 4,\ 2 \wedge 3,\ 2 \wedge 4,\ 3 \wedge 4) = (1, 2, 3, 4, 5, 6).$$

Suppose that $\boldsymbol{y}$ and $\tilde{\boldsymbol{y}}$ are both solutions of the linear system

$$\boldsymbol{y}' = B\boldsymbol{y} \tag{4.21}$$

where the matrix-valued B has columns $\boldsymbol{b}_j$, $j = 1, \ldots, n$. Then since $B\boldsymbol{y} = \sum y_j \boldsymbol{b}_j$, one computes that $\hat{\boldsymbol{y}} := \boldsymbol{y} \wedge \tilde{\boldsymbol{y}}$ satisfies the linear system

$$\hat{\boldsymbol{y}}' = (B_\wedge)\hat{\boldsymbol{y}} \tag{4.22}$$

where matrix $B_\wedge$ has columns given by $\hat{\boldsymbol{b}}_{j \wedge k} = \boldsymbol{b}_j \wedge \boldsymbol{e}_k + \boldsymbol{e}_j \wedge \boldsymbol{b}_k$. The system in (4.22) is called the *exterior system* associated with (4.21). Similarly, for two solutions $\boldsymbol{z}$ and $\tilde{\boldsymbol{z}}$ of the adjoint system

$$\boldsymbol{z}' = -\boldsymbol{z}B$$

the exterior product $\hat{\boldsymbol{z}} := \boldsymbol{z} \wedge \tilde{\boldsymbol{z}}$ is a solution to the associated exterior system

$$\hat{\boldsymbol{z}}' = -\hat{\boldsymbol{z}}(B_\wedge). \tag{4.23}$$

It is a straightforward matter to compute that

$$(\boldsymbol{z} \wedge \tilde{\boldsymbol{z}}) \cdot (\boldsymbol{y} \wedge \tilde{\boldsymbol{y}}) = \det \begin{pmatrix} \boldsymbol{z} \cdot \boldsymbol{y} & \boldsymbol{z} \cdot \tilde{\boldsymbol{y}} \\ \tilde{\boldsymbol{z}} \cdot \boldsymbol{y} & \tilde{\boldsymbol{z}} \cdot \tilde{\boldsymbol{y}} \end{pmatrix}. \tag{4.24}$$

As a consequence of (4.24) and Proposition 4.5, the Evans function E_j may be expressed as

$$E_j(\lambda) = (\boldsymbol{z}_1^{(\infty)} \wedge \boldsymbol{z}_2^{(\infty)}) \cdot (\boldsymbol{y}_1^{(0)} \wedge \boldsymbol{y}_2^{(0)}). \tag{4.25}$$

This expression has advantages for both theoretical and numerical purposes, which stem from the fact that the exterior products $\boldsymbol{z}_1^{(\infty)} \wedge \boldsymbol{z}_2^{(\infty)}$ and $\boldsymbol{y}_1^{(0)} \wedge \boldsymbol{y}_2^{(0)}$ have a separate characterization that shows they are independent of any particular choice of the individual solutions involved.

Proposition 4.6 *Fix an integer $m \neq 0$, the base wave radial profile w, the index j, and a complex number $\lambda \in \mathbb{C}_\sigma$. The exterior system associated with (4.6) has a unique solution $\hat{\boldsymbol{y}}^{(0)}(r, \lambda)$ with the asymptotic behavior*

$$\hat{\boldsymbol{y}}^{(0)} \sim \mathring{\boldsymbol{y}}_1 \wedge \mathring{\boldsymbol{y}}_2 \quad \text{as } r \to 0^+.$$

Similarly, the exterior system associated with the adjoint system (4.13) has a unique solution $\hat{\boldsymbol{z}}^{(\infty)}(r, \lambda)$ with the asymptotic behavior

$$\hat{\boldsymbol{z}}^{(\infty)} \sim \mathring{\boldsymbol{z}}_1 \wedge \mathring{\boldsymbol{z}}_2 \quad \text{as } r \to \infty.$$

Furthermore, the solutions $\hat{\boldsymbol{y}}^{(0)}(r, \lambda)$, $\hat{\boldsymbol{z}}^{(\infty)}(r, \lambda)$ are analytic functions of λ globally in the cut plane $\mathbb{C}_\sigma$.

Corollary 4.7 *For any choice of solutions $\boldsymbol{y}_k^{(0)}$, $\boldsymbol{y}_k^{(\infty)}$, $\boldsymbol{z}_k^{(\infty)}$ having the properties indicated in Lemmas 4.1 and 4.4 we have*

$$\boldsymbol{y}_1^{(0)} \wedge \boldsymbol{y}_2^{(0)} = \hat{\boldsymbol{y}}^{(0)}, \quad \boldsymbol{z}_1^{(\infty)} \wedge \boldsymbol{z}_2^{(\infty)} = \hat{\boldsymbol{z}}^{(\infty)}.$$

The Evans function E_j is given by

$$E_j(\lambda) = \hat{\boldsymbol{z}}^{(\infty)} \cdot \hat{\boldsymbol{y}}^{(0)}, \tag{4.26}$$

and E_j is analytic globally in the cut plane $\mathbb{C}_\sigma$.

The proof of Proposition 4.6 is in Appendix C.2. The uniqueness property of the solution $\hat{\boldsymbol{y}}^{(0)}$ with the given asymptotic normalization stems from the fact that it is a solution of the exterior system associated with (4.6) having *maximal decay rate* as $r \to 0$. Similarly, $\hat{\boldsymbol{z}}^{(\infty)}$ is a solution of the adjoint exterior system having maximal decay rate as $r \to \infty$.

Corollary 4.7 follows from Proposition 4.6 via the observation that $\boldsymbol{y}_1^{(0)} \wedge \boldsymbol{y}_2^{(0)}$ and $\boldsymbol{z}_1^{(\infty)} \wedge \boldsymbol{z}_2^{(\infty)}$ are solutions of the exterior systems associated with (4.6) and (4.13), respectively, with the asymptotic behaviors given in Proposition 4.6. Thus both $\boldsymbol{y}_1^{(0)} \wedge \boldsymbol{y}_2^{(0)}$ and $\boldsymbol{z}_1^{(\infty)} \wedge \boldsymbol{z}_2^{(\infty)}$ are globally analytic functions of λ in $\mathbb{C}_\sigma$, and it follows from (4.25) that E_j is given by (4.26) and is also globally analytic in $\mathbb{C}_\sigma$.

5 Numerical computation and results

5.1 Evaluation of Evans functions

To evaluate the Evans function $E_j(\lambda)$ in (4.12) for given j and λ, we use a Runge-Kutta ODE package (rksuite) to compute numerical approximations to the solutions $\boldsymbol{y}_1^{(0)}(r)$ and $\boldsymbol{y}_2^{(0)}(r)$ of (4.6) that are bounded at the origin. To do this, we solve two initial value problems for the system (4.6)

on an interval $r_0 \le r \le r_\infty$, where r_0 and r_∞ are chosen so that $w(r)$ is small (usually $< 10^{-4}$) on $(0, r_0)$ and (r_∞, ∞). Then $\alpha(w(r))$ and $\beta(w(r))$ are close to their asymptotic values on the intervals $(0, r_0)$ and (r_∞, ∞). We make the approximations $\boldsymbol{y}_i^{(0)}(r_0) \approx \mathring{\boldsymbol{y}}_i(r_0)$ $(i = 1, 2)$ to determine the initial conditions. We then evaluate the Wronskian of the computed approximations to $\boldsymbol{y}_1^{(0)}(r_\infty)$ and $\boldsymbol{y}_2^{(0)}(r_\infty)$ with the explicitly known approximations $\mathring{\boldsymbol{y}}_3(r_\infty)$ and $\mathring{\boldsymbol{y}}_4(r_\infty)$ to the respective values $\boldsymbol{y}_3^{(\infty)}(r_\infty)$ and $\boldsymbol{y}_4^{(\infty)}(r_\infty)$ of the solutions to the system (4.6) that vanish at infinity.

Our actual numerical implementation of this scheme makes use of a change of variables and scaling to reduce the sometimes rapid variation of solutions and improve the quality of the computation. We represent a solution $\boldsymbol{y}(r)$ of the system (4.6) as an r-dependent scaled linear combination of the basis elements $\left\{ \mathring{\boldsymbol{y}}_i : i = 1, \dots, 4 \right\}$ for the asymptotic system (4.8), writing

$$\boldsymbol{y}(r) = \mathring{\boldsymbol{Y}}(r) \exp(\boldsymbol{K} r) \boldsymbol{b}(r) \tag{5.1}$$

where $\boldsymbol{K} := \operatorname{diag}\{-k_+, -k_-, k_+, k_-\}$, Then we can anticipate that the vector $\boldsymbol{b}(r)$ is well-behaved as r becomes large, and it satisfies the system

$$\boldsymbol{b}'(r) = \boldsymbol{D}(r) \boldsymbol{b}, \tag{5.2}$$

whose coefficient matrix $\boldsymbol{D}(r) = -\boldsymbol{K} + e^{-Kr} \mathring{\boldsymbol{Y}}^{-1}(r) \tilde{\boldsymbol{B}}(r) \mathring{\boldsymbol{Y}}(r) e^{Kr}$ remains bounded as $r \to \infty$.

The Evans functions $E_j(\lambda)$ are also approximated in a similar but simpler way based on the expression in (4.26), by computing an approximation to $e^{-kr} \hat{\boldsymbol{y}}^{(0)}(r)$ for $r_0 \le r \le r_\infty$ and using the known asymptotic approximation for $\hat{\boldsymbol{z}}^{(\infty)}(r_\infty)$. The scaling factor k is given by $k = k_+ + k_-$. Numerical convergence studies indicate that we usually attain 8 to 10 digit accuracy with this approach. This method of evaluating $E_j(\lambda)$ is very stable, since $\hat{\boldsymbol{y}}^{(0)}$ is a solution of the exterior system with maximal asymptotic growth rate. It also avoids a potential difficulty one can encounter with the Wronskian approach — maintaining the linear independence of approximations to $\boldsymbol{y}_1^{(0)}$ and $\boldsymbol{y}_2^{(0)}$ is difficult if the growth rates for these solutions differ greatly and if the interval of computation is large.

5.2 Counting eigenvalues with the argument principle

Let us first recall what is known about the possible location of unstable eigenvalues. According to Proposition 3.3 we may locate eigenvalues of A by locating zeros of the Evans functions $E_j(\lambda)$. For a given standing wave $u_0 = e^{i\omega t} e^{im\theta} w(r)$, Proposition 3.5 guarantees that all such zeros lie in the strip where

$$|\operatorname{Re} \lambda| \le \Lambda_{\max} := \max_{r \ge 0} (|\alpha(w(r))| + |\beta(w(r))|). \tag{5.3}$$

Theorem 3.4 guarantees that all unstable eigenvalues λ will be zeros of E_j with

$$|j| \le j_{\max} := |m| + \max_{r \ge 0} \sqrt{r^2 (\alpha(w(r)) + |\beta(w(r))|)} \, . \tag{5.4}$$

Furthermore, it follows from Proposition 4.3 that $E_{-j}(\lambda) = 0$ if and only if $E_j(\bar{\lambda}) = 0$, so that zeros of E_{-j} in the strip $0 < \operatorname{Re} \lambda \le \Lambda_{\max}$ are in one-to-one correspondence with zeros of E_j in that strip.

To search for zeros of the Evans functions in the strip $|\operatorname{Re} \lambda| \le \Lambda_{\max}$, we apply the argument principle to count the number of zeros of the analytic functions E_j inside a contour that encloses a "large" part of the strip. We do not have a rigorous bound on $|\operatorname{Im} \lambda|$ for unstable eigenvalues, but in practice we find that $|E_j(\lambda)|$ grows for large $|\lambda|$, so we take a large contour determined so that an asymptotic trend appears established. Figure 7 shows a schematic of the contour γ employed in our computations, lying in the cut plane $\mathbb{C}_\sigma$. The contour is designed to enclose the region where

$|\operatorname{Re}\lambda| \le \Lambda_{\max}$ and $|\operatorname{Im}\lambda| \le K$, except for an ϵ-neighborhood of the essential spectrum $\{it \mid |t| \ge \sigma^2\}$. The parameter ϵ is taken small ($\approx 10^{-6}$), and K large.

Using the computed approximation to $E_j(\lambda)$ for given j and λ described above, we compute the winding number of the image $E_j(\gamma)$ about 0. This is the change in the argument of the complex number $E_j(\lambda)$ as λ traverses the curve γ, divided by 2π. We use an adaptive stepping procedure to traverse γ in steps that result in a small relative change in $E_j(\lambda)$, and accumulate the change in $\arg E_j(\lambda)$. By the argument principle, this yields the number of zeros of E_j enclosed by γ.

Because of the symmetry $E_j(-\bar{\lambda}) = \overline{E_j(\lambda)}$ from Proposition 4.3(iii), in practice we need only to compute the change in argument of $E_j(\lambda)$ along the portion γ_r of the contour γ in the right-half plane $\operatorname{Re}\lambda \ge 0$. Doubling yields the total change in argument along γ.

By the same symmetry, the number of zeros enclosed by γ in the right half-plane is the same as the number in the left half-plane. So, from the winding number above, we need to subtract the number of purely imaginary zeros and divide by two to determine the number of *unstable* eigenvalues of A corresponding to index j enclosed by γ. To find the purely imaginary zeros we exploit the fact established in Proposition 4.3 that $E_j(\lambda)$ is real if λ is purely imaginary. We plot the real function $E_j(it)$ for $t \in [-\sigma^2 + \epsilon, \sigma^2 - \epsilon]$, refining and checking the multiplicity of zeros with log-log plots as necessary.

The computation of the winding number can be considerably slowed by the presence of zeros of $E_j(\lambda)$ very near the contour — the adaptive stepping procedure takes small steps to track the image curve near such a zero. The reason we do not take our contour to be a simple rectangle with one side along $\operatorname{Re}\lambda = \epsilon$ is to avoid passing near numerous zeros on the imaginary axis between $-i\sigma^2$ and $i\sigma^2$.

Nevertheless, it sometimes happens that the values of $E_j(\lambda)$ become small as λ traverses the part of the contour γ_r in the right half-plane near the essential spectrum on the imaginary axis. This behavior suggests that the contour passes near a zero of E_j. To verify that these zeros do not lie in the right half-plane outside γ, we use low-degree least-square polynomial fits to extrapolate an approximation to $E_j(\lambda)$ near γ_r, and a root finder to locate the zeros. In all cases the zeros appear to lie in the left half-plane. In view of the symmetry $\overline{E_j(\lambda)} = E_j(-\overline{\lambda})$, we interpret these findings to indicate not that E_j has zeros in the cut plane $\mathbb{C}_\sigma$ outside γ, but rather that the analytic continuation of $E_j(\lambda)$ across the imaginary axis has zeros near the axis. Such points are known as *resonance poles*, see [26].

5.3 Spinless ground-state waves

The stability of ground state (nodeless) standing-wave solutions to (1.1) with nonlinearities that include those we consider here is analyzed in [13] and [34]. These works establish that a family of ground state standing waves ($m = n = 0$), parametrized by standing wave frequency ω, is orbitally stable (stable modulo spatial translations and phase shifts under H^1 perturbations of initial data) if $dN/d\omega > 0$ and unstable (to radial perturbations) if $dN/d\omega < 0$, where $N = \|u_0\|^2$. For general nonlinearities, the stability of the ground state in the marginal case $dN/d\omega = 0$ is open, but for pure-power nonlinearities $g(u) = \gamma|u|^{p-1}u$ (for which $dN/d\omega = 0$ is equivalent in d spatial dimensions to $p = 1 + 4/d$) the ground state is unstable in the sense that there exist arbitrarily small L^2 perturbations of initial data for which the corresponding solution of (NLS) blows up in H^1 norm in finite time. (See [32].)

The construction and computation of the Evans functions for these spinless waves differs from the description we have given above, since the wave amplitude $w(r)$ approaches a nonzero value as r approaches zero. Nevertheless, through diagonalization of the coupling matrix in (3.15), explicit (formal) asymptotic solutions may be written and Evans functions computed. For brevity we omit the details, since our primary concern is the spectral stability of standing waves with spin.

We performed computations for spinless waves for the cubic and cubic-quintic nonlinearities, both to validate the numerical code and to study the mechanism of transition to instability as the

quantity $dN/d\omega$ changes sign.

The cubic nonlinear Schrödinger equation in two spatial dimensions is a marginal case from the point of view of theory ($dN/d\omega = 0$). Recall that by scaling we may without loss of generality take $g(u) = |u|^2u$ and consider only the fixed standing wave frequency $\omega = 1$. The bounds from Theorem 3.4 and Proposition 3.5 yield that $|j| \le j_{\max} = 1.85$ and $|\operatorname{Re}\lambda| \le 14.6$ for unstable eigenvalues. In fact we find no eigenvalues with positive real part, indicating that the mechanism for instability in this case is not exponential linear instability. The eigenvalue $\lambda = 0$ has high multiplicity, however — it is found to be a zero of E_j of order 4 for $j = 0$ and of order 2 for $j = 1$. (This remains true for the cubic for all spin/node-number combinations considered.) This order is consistent with the enumeration of zero modes in Appendix B. No other discrete eigenvalues are found.

To study transition to instability, we perturb the cubic nonlinearity and analyze the one-parameter family $g(u) = |u|^2u - \delta|u|^4u$. Making use of the scaling transformation $w(r) = \sqrt{\omega}\tilde{w}(\sqrt{\omega}\,r)$, we may without loss of generality study eigenvalues for the single standing-wave frequency $\omega = 1$. For the wave to exist, δ must satisfy $\delta < \frac{3}{16}$. Numerical computation of $N = 2\pi\int_0^\infty w(r)^2 r\,dr$ for the wave profiles indicates that, by the stability criterion for ground states, u_0 is stable ($dN/d\omega > 0$) for $0 < \delta < \frac{3}{16}$ and is unstable ($dN/d\omega < 0$) for $\delta < 0$.

Our numerical search for eigenvalues shows that the transition to instability of the ground state as δ decreases through zero is characterized by the collision of two purely imaginary conjugate eigenvalues in the twist-0 ($j = 0$) subspace. We observe the transition by plotting $E_0(i\tau)$ for $\tau \in (-\sigma^2, \sigma^2)$ for various values of δ. For $0 < \delta < \frac{3}{16}$, log-log plots indicate that the function $E_0(i\tau)$ has a zero of multiplicity two at $\tau = 0$ and two other conjugate simple zeros. As $\delta \to 0^+$, the simple zeros approach $\tau = 0$, and at $\delta = 0$ there is a zero of multiplicity four at $\tau = 0$. For $\delta < 0$, two real zeros of $E_0(\lambda)$ emerge with opposite sign on the real axis. This creates a positive eigenvalue that renders the standing wave exponentially unstable.

5.4 Waves with nodes

In all our computations for "first excited states," waves whose profiles have a single node where $w(r) = 0$ for some $r > 0$, we find many unstable eigenvalues. This holds whether the waves have spin or not. For example, for the cubic with $m = 0$, $n = 1$, we find 12 unstable eigenvalues, distributed as $(2, 1, 1, 1, 1, 1, 0\ldots)$, which we abbreviate as $(2, 1(5\times), 0\ldots)$, meaning two in index $j = 0$ and one each in index j for $|j| = 1, \ldots, 5$. For $m = 1$, we find 24 unstable eigenvalues, distributed as $(2(4\times), 1(5\times), 0\ldots)$. For $m = 2$, we find 34, distributed as $(2(6\times), 1(6\times), 0\ldots)$. The existence of eigenfunctions with twist $j = 0$ leads us to expect that the higher-node-number states have exponential instabilities to perturbations of initial data of the form $e^{im\theta}v(r)$. For the cubic-quintic $g(u) = |u|^2u - |u|^4u$ we only mention a few cases with $n = 1$ since now different values of ω are in principle different: with $m = 0$, $\omega = 0.05$ we find 10 unstable eigenvalues; with $m = 1$, $\omega = 0.16$ we find 20; and with $m = 2$, $\omega = 0.165$ we find 24. It proved difficult to perform accurate computations for profiles with more than one node ($n > 1$), but we expect all such waves to be unstable.

5.5 Spinning waves with no nodes

For the cubic nonlinearity (scaled so $\omega = 1$) our numerical results indicate that spinning standing waves with no nodes ($n = 0$) are unstable. With spin $m = 1$, there are 6 unstable eigenvalues[1], one for each twist index with $|j| = 1, 2, 3$. And there are 8 eigenvalues in the "gap" $\{it \mid -\sigma^2 < t < \sigma^2\}$, distributed in j as $(4, 2, 1, 0, 1, 0\ldots)$. For $m = 2$, there are 6 unstable, one for each $j = 1, \ldots, 6$, with 11 gap eigenvalues distributed as $(4, 2, 1, 1, 1, 0, 0, 1, 1, 0\ldots)$.

[1] $1.17 \pm 1.52i$, $1.97 \pm 1.69i$, $1.81 \pm 1.88i$

Table 1: Eigenvalue distribution and bounds at the instability transition for the cubic-quintic nonlinearity. Waves with spin m are spectrally stable for $\omega_{\rm cr} \le \omega < \omega_*$. Unstable eigenvalues emerge at $\lambda_{\rm cr}$, and can exist only for $|j| \le j_{\max}$ by Theorem 3.4.

m	$\omega_{\rm cr}$	$\lambda_{\rm cr}$	$j_{\max}$	# of zeros in gap, for $j = 0, 1, \dots$
1	0.1487	$0.0478i$	7.66	$4, 3, 3, 2, 1, 0 \dots$
2	0.1619	$0.0271i$	14.2	$4, 4, 3(4\times), 1(4\times), 0 \dots$
3	0.1700	$0.0136i$	23.4	$4, 4, 5, 5, 4, 3(4\times), 2, 1(5\times), 0 \dots$
4	0.1769	$0.0063i$	38.3	$6(5\times), 5(4\times), 3(7\times), 2, 1(7\times), 0 \dots$
5	0.1806	$0.0033i$	57.6	$8(3\times), 7(6\times), 6, 5(4\times), 3(10\times), 2(3\times), 1(10\times), 0 \dots$

Next we consider the cubic-quintic nonlinearity $g(u) = \gamma|u|^2u - \delta|u|^4u$, where the constants γ and δ are both positive. As mentioned in section 2, the scaling $w(r) = \sqrt{\frac{\gamma}{\delta}}\,\tilde{w}(\frac{\gamma}{\sqrt{\delta}}r)$ allows us to suppose without loss of generality that $\gamma = \delta = 1$. The allowable range for ω, for which $F(s) > 0$ for some $s > 0$, is $0 < \omega < \omega_* = \frac{3}{16}$.

Spectrally stable waves. For the nodeless waves with spins $m = 1, 2, 3, 4, 5$, we have discovered ranges of standing-wave frequency ω for which all the Evans functions E_j, $j = 0, 1, \dots, j_{\max}$, appear to have no zeros with positive real part. Our numerical computations indicate that, for a given value of spin m, there is a transition frequency $\omega_{\rm cr}$ such that A possesses unstable eigenvalues for $0 < \omega < \omega_{\rm cr}$ but A has no unstable eigenvalues for $\omega_{\rm cr} < \omega < \omega_*$. In Table 1 we list the transition frequency $\omega_{\rm cr}$, the bound on instability index from Theorem 3.4 and the computed distribution of all purely imaginary gap eigenvalues. The figures in parentheses indicate the number of times a count is repeated, so that "$8(3\times), 7(6\times)$" in the last row of the table means that there are 8 gap eigenvalues for each $j = 0, 1, 2$, and 7 eigenvalues for each $j = 3, 4, 5, 6, 7, 8$. Accordingly, the total number of gap eigenvalues for $m = 1, 2, 3, 4, 5$ respectively is 22, 44, 78, 154, 268. The bound computed from Lemma 3.5 on the real part of any unstable eigenvalue satisfies $\Lambda_{\max} < 1$ in all cases. The value $\lambda = 0$ is always found to be a double zero of E_j for $j = 0$ and 1, which corresponds to the four zero modes enumerated in Appendix B.

For each $m = 1, \dots, 5$ the mechanism for transition to instability as ω decreases below $\omega_{\rm cr}$ is the same. A pair of purely imaginary gap eigenvalues, always with index $j = 2$, collides when $\omega = \omega_{\rm cr}$ at $\lambda = \lambda_{\rm cr}$ (as shown in Table 1) and move away from the imaginary axis in opposite directions, creating an unstable eigenvalue. Figure 8 shows how the graph of the real-valued function $E_2(it)$ $(-\omega < t < \omega)$ changes as ω passes through the critical frequency for the case of spin $m = 1$. Figure 9 shows the critical wave profiles for $m = 1, \dots, 5$.

Figure 10 shows a log-log plot of $\omega_{\rm cr}$ versus m. (The transition frequency is calculated for noninteger values of m by solving the profile equation (1.4) and computing the associated Evans functions.) From this data it appears that

$$\omega_* - \omega_{\rm cr} \sim \frac{0.18}{m^2} \tag{5.5}$$

as m becomes large, suggesting that stable spinning waves may exist for any spin m.

After this paper was submitted, the existence of a stability transition frequency $\omega_{\rm cr}$ for $m = 1$ and 2 was also reported in a paper of Towers *et al.* [31], who solve numerically the algebraic eigenvalue problem arising from discretization of a system of equations equivalent to (3.15). These authors also report finding (at the limit of their numerical accuracy) a weak instability for $j = \pm 1$ (see Figure 5 in [31]) which affects the location of $\omega_{\rm cr}$ for $m = 1$ and 2 and causes them to find all waves with $m = 3$ unstable. If our present numerical results are correct, this weak instability is likely to be a numerical artifact, since for $j = 1$ the existence of a double eigenvalue at $\lambda = 0$ is consistent with the analysis of zero modes in Appendix B, and we find no other zeros of $E_1(\lambda)$ inside or near the

contour γ except on the imaginary axis, where $E_j(\lambda)$ is real and changes of sign clearly locate zeros.

We examined a few cases involving nonlinearities other than cubic and cubic-quintic to see whether spectrally stable localized standing waves may exist. For the focusing-defocusing nonlinearity $g(w) = w^3 - w^7$, the critical frequency at which F has two zero-height hilltops is $\omega_* \approx 0.2722$. Our computations indicate that the wave with spin $m = 1$ for $\omega = 0.24$ is spectrally stable ($j_{\max} = 9$ and $|\operatorname{Re}\lambda| < 0.91$ for unstable eigenvalues in this case). For the focusing-defocusing nonlinearity $g(w) = w^5 - w^7$, the critical frequency $\omega_* \approx 0.0878$, and there is a spectrally stable wave with spin $m = 1$ for $\omega = 0.07$ ($j_{\max} = 11$ and $|\operatorname{Re}\lambda| < 1.27$).

For the saturable nonlinearity $g(w) = w^3/(1 + w^2)$, which is always focusing, we found no spectrally stable spinning waves. Spinning solitary waves exist for $0 < \omega < 1$, growing in amplitude without bound as ω increases. With spin $m = 1$, we find for small ω that there are three unstable eigenvalues, as in the case of the focusing cubic above. For $\omega \geq 0.35$, however, we find only one unstable eigenvalue; it has twist index $j = 2$. And as ω increases towards 1, the real part of the unstable eigenvalue becomes small. E.g., for $\omega = 0.5$ the unstable eigenvalue is $\lambda = 0.174 + 0.199i$, and for $\omega = 0.9$ it is $0.0372 + 0.0547i$. As ω increases, then, we see that the nonlinearity saturates and the wave becomes less unstable.

6 Discussion

Our computations support the conjecture that for any focusing-defocusing nonlinearity, solitary waves with spin (encapsulated vortices) are spectrally stable for any value of the spin index m if they have no nodes ($n = 0$) and if the standing wave frequency ω is sufficiently close to the kink frequency ω_*, which is determined by the property that the graphs of $y = g(x)$ and $y = \omega_* x$ enclose two regions of equal area for $0 \leq x \leq a_*$. (Equivalently, the potential $F = F(s)$ has two zero-height maxima, at $s = 0$ and $s = a_*$.)

To begin to understand why these waves might be stable, we observe that in the regime when $\omega \approx \omega_*$ and $|m|$ is large, the wave profiles develop a structure that may be accessible to analysis. This structure is suggested from Figures 4 and 6, and a formal analysis is given in Appendix A. In this regime, the wave amplitude $w(r)$ is approximately zero in a large central core region, then rises quickly in a transition layer where $r \approx R_{\text{in}}$ to a wide region where $w(r) \approx a_*$, then decreases rapidly in a transition layer where $r \approx R_{\text{out}}$ to zero.

Since the wave amplitude remains approximately constant near a_* in a wide annular region where r is large and θ is slowly varying, the solution is slowly varying in space. Now because the nonlinearity is defocusing for amplitudes near a_* ($h' < 0$) the spatially constant solution $u = a_* e^{i\omega_* t}$ is spectrally stable, by remark 3.2. The zero solution is also spectrally stable, but spatially constant solutions with amplitude in the focusing range $0 < a < a_0$ are not spectrally stable.

In the zones of rapid transition where r is large and θ slowly varying, the wave profiles $w(r)$ appear to be well-approximated by a one-dimensional kink solution of the nonlinear Schrödinger equation (1.1). Such a solution has the form $\gamma e^{i\omega_* t}\phi_*(x)$, where ϕ_* is as described in section 2 and where γ is a complex constant of unit modulus. This kink connects the zero solution to the solution $\gamma a_* e^{i\omega_* t}$. It is significant to note that the kink solution itself is a spectrally stable solution of (1.1). Because of the invariance of (1.1), we may take $\gamma = 1$ in analyzing the stability of $\gamma e^{i\omega_* t}\phi_*$.

Proposition 6.1 *Assume that $g(u) = h(|u|^2)u$ where h is C^1 with $h(0) = 0$, and that properties (i) and (ii) of the introduction hold. Then (1.1) admits a one-dimensional kink solution $u(x, y, t) = e^{i\omega_* t}\phi_*(x)$, where ϕ_* is the unique solution of (2.7) and (2.8), and this solution is spectrally stable.*

Proof The existence and uniqueness of ϕ_* are easy to establish. To analyze the stability, we perform the linearization of section 3 for $u_0(x, y, t) = e^{i\omega_* t}\phi_*(x)$, obtaining $\partial_t \Psi = A\Psi$, where now

$$A = J\left(\Delta - \sigma^2 + \alpha(\phi_*(x)) + \beta(\phi_*(x))R\right). \tag{6.1}$$

Taking the Fourier transform in the transverse variable y, we obtain $\partial_t \hat{\Psi} = \hat{A}\hat{\Psi}$ with $\hat{A} = -J(L+\ell^2 I)$, where ℓ is the Fourier transform variable and

$$L = \begin{pmatrix} L_+ & 0 \\ 0 & L_- \end{pmatrix} = \begin{pmatrix} -\partial_x^2 - f_*'(\phi_*) & 0 \\ 0 & -\partial_x^2 - f_*(\phi_*)/\phi_* \end{pmatrix}. \tag{6.2}$$

Consider the spectrum of L. We know $f_*'(0) < 0$, $f_*'(a_*) < 0$, and $f_*(a_*) = 0$, therefore

$$\lim_{x\to\pm\infty} f_*'(\phi_*(x)) < 0 \quad \text{and} \quad \lim_{x\to\pm\infty} f_*(\phi_*(x))/\phi_*(x) \le 0.$$

Hence the essential spectra of L_+ and L_- are contained in $[0,\infty)$. Each operator L_+ and L_- annihilates a function of definite sign:

$$L_-\phi_* = 0 \qquad \text{and} \qquad L_+\phi_*' = 0,$$

so a standard argument based on the maximum principle implies that L_+ and L_- have no negative eigenvalues. Thus $L + \ell^2 I$ has no negative eigenvalues, and it is simple to show that then $J(L+\ell^2)$ has no eigenvalues with nonzero real part. It follows that the spectrum of A is purely imaginary. Thus the kink $e^{i\omega_* t}\phi_*(x)$ is spectrally stable, as claimed. □

The focusing-defocusing properties of the nonlinearity thus permit the existence of a spectrally stable one-dimensional kink.

A simplified description of the wave amplitude profiles, for spinning solitary waves when $\omega \approx \omega_*$ and $|m|$ is large, is that they have two pieces:

(i) an outer kink region where $w(r) \approx \phi_*(r - R_{\rm out})$,

(ii) an inner kink region where $w(r) \approx \phi_*(R_{\rm in} - r)$.

Both the inner and outer kink radii $R_{\rm in}$ and $R_{\rm out}$ become large, with $R_{\rm out}$ much larger that $R_{\rm in}$. Since both pieces approximate a spectrally stable one-dimensional kink solution, it becomes plausible that the whole wave can be stable.

A Asymptotic analysis of wave structure

As indicated in section 2, here we formally analyze the structure of nodeless localized waves in two limiting regimes, namely (i) when the spin m becomes arbitrarily large, and (ii) when the nonlinearity is of "hilltop" type and the standing wave frequency ω approaches the critical value ω_* at which the positive maximum value of the potential F becomes zero, i.e., becomes equal to the local maximum at 0.

A.1 Nodeless wave location for large spin index m

We observe numerically that the nodeless standing wave profiles w for large values of m appear to be copies of a single profile, shifted further to the right as m increases. To understand and characterize this property, we note that r is large where the wave amplitude is non-negligible. The term w'/r in (1.4) is thus apparently negligible, and we surmise that the quantity m^2/r^2 is approximately constant where the wave amplitude is non-negligible.

We therefore conjecture that $w(r) \approx \phi_A(r - R)$, where ϕ_A is a putative positive solution to

$$\phi'' - A\phi + f(\phi) = 0 \tag{A.1}$$

with maximum at the origin, that vanishes as $r \to \pm\infty$, and where $A = m^2/R^2$, with R to be determined. Since $A > 0$ and $f'(0) < 0$, the solution ϕ_A, if it exists, has exponential decay as

$|r| \to \infty$. Energy considerations show that such a solution ϕ_A will exist provided that the even function $F_A(s) \equiv F(s) - \frac{1}{2}As^2$ has a positive zero.

To determine R or equivalently A, we derive an identity valid for profiles. Multiplying the equation (1.4) by w' and rearranging terms, we obtain

$$\frac{1}{r}w'^2 - \frac{m^2}{r^3}w^2 + \left[\frac{1}{2}w'^2 - \frac{m^2}{2r^2}w^2 + F(w)\right]' = 0. \tag{A.2}$$

Because $w(r) \sim dr^m$ as $r \to 0^+$, if $m \geq 1$ the quantity in square brackets vanishes as $r \to 0^+$, and it also vanishes as $r \to \infty$. Integrating (A.2), we find

$$\int_0^\infty \left(\frac{1}{r}w'^2 - \frac{m^2}{r^3}w^2\right) dr = 0 \tag{A.3}$$

for $m \geq 1$.

Approximating r in the integrand of (A.3) by R, we find

$$A\int_0^\infty \phi_A(r-R)^2\, dr \approx \int_0^\infty \phi_A'(r-R)^2\, dr. \tag{A.4}$$

Extending the integration to the whole line, we arrive at the approximation

$$A\int_{-\infty}^\infty \phi_A(x)^2\, dx \approx \int_{-\infty}^\infty \phi_A'(x)^2\, dx. \tag{A.5}$$

We may compute the values of these integrals in terms of A by quadrature, as follows. Assume that F_A has a positive zero, and let B be the smallest positive zero of the function F_A. (That is, B is the solution to $F(B) = \frac{1}{2}AB^2$.) If $\phi(r)$ is a solution to (A.1), then the energy $E[\phi] = \frac{1}{2}\phi'(r)^2 + F_A(\phi(r))$ is independent of r. It follows from the facts that $F_A(0) = 0$ and $\phi_A(r) \to 0$ as $r \to \infty$ that $E[\phi_A] = 0$ and hence that the turning point of the solution ϕ_A at $r = 0$ occurs at amplitude $\phi_A(0) = B$. Furthermore, we may solve $E = 0$ for ϕ' to obtain

$$|\phi_A'| = \sqrt{-2F_A(\phi_A)}. \tag{A.6}$$

By changing variables from r to $p = \phi_A(r)$, we find that

$$\int_0^\infty \phi_A'(r)^2\, dr = \int_0^B \sqrt{-2F_A(p)}\, dp, \tag{A.7}$$

$$\int_0^\infty \phi_A(r)^2\, dr = \int_0^B \frac{p^2}{\sqrt{-2F_A(p)}}\, dp. \tag{A.8}$$

Since ϕ_A is an even function we may double these values to obtain the values of the integrals over the whole line. The resulting expressions inserted into (A.5) yield an equation that determines A.

As an example, we consider the cubic nonlinearity $F(s) = -s + s^3$. We have $F_A(\phi) = \frac{1}{4}\phi^4 - \frac{1}{2}(1+A)\phi$, hence $B = \sqrt{2(1+A)}$ and

$$\int_0^\infty \phi_A'(r)^2\, dr = \int_0^{\sqrt{2(1+A)}} \sqrt{(1+A)p^2 - \tfrac{1}{2}p^4}\; dp = \tfrac{2}{3}(1+A)^{3/2} \tag{A.9}$$

and

$$\int_0^\infty \phi_A(r)^2\, dr = \int_0^{\sqrt{2(1+A)}} \frac{p^2}{\sqrt{(1+A)p^2 - \frac{1}{2}p^4}}\, dp = 2\sqrt{1+A}. \tag{A.10}$$

Therefore, in this example, equation (A.5) yields $A = \frac{1}{2}$, and we predict that the large-m profile will be centered at $R = \sqrt{2}\, m$ and will have amplitude $B = \sqrt{3}$. This agrees well with the data shown in Fig. 3. We remark that in this example the values of the integrals in (A.5) can also be determined from the explicit formula $\phi_A(x) = \sqrt{2(1+A)}\,\mathrm{sech}(\sqrt{1+A}\,x)$.

A.2 Kink location in the flattop regime

Here we study the structure of localized waves for "hilltop" potentials such as arise for the cubic-quintic in (1.2), when ω approaches the critical value ω_* from below. For ω near ω_*, in the cubic-quintic case we observe numerically that the nodeless wave profile $w(r)$ remains near $w_{\max} \approx a_*$ in a large interval, then decreases rapidly to zero when r is near the last point R where $w(R) = \frac{1}{2}a_*$. Near this point the profile $w(r)$ seems well-approximated by $\phi_*(r-R)$, where ϕ_* is the decreasing kink solution to (2.7) that satisfies (2.8).

To approximately determine R, we return to the identity (A.2) and integrate from $R-X$ to $R+X$ to obtain

$$\int_{R-X}^{R+X} \left(\frac{1}{r}w'^2 - \frac{m^2}{r^3}w^2\right)\,dr = -\left[\frac{1}{2}w'^2 - \frac{m^2}{2r^2}w^2 + F(w)\right]\Bigg|_{R-X}^{R+X}. \tag{A.11}$$

We fix X large compared to 1 but independent of R.

We first approximate the left side of (A.11). Because $w'(r)$ is nonnegligible only for $r \approx R$, and because $w(r) \approx 0$ for $r > R$ and $w(r) \approx a_*$ for $r < R$, we have

$$\int_{R-X}^{R+X} \left(\frac{1}{r}w'^2 - \frac{m^2}{r^3}w^2\right)\,dr \approx \frac{1}{R}\int_{R-X}^{R+X} w'^2\,dr - m^2(a_*)^2\int_{R-X}^{R}\frac{1}{r^3}\,dr. \tag{A.12}$$

We now approximate $w'(r)$ in the integrand by ${\phi_*}'(r-R)$, and extend the integration to the whole line. Setting

$$T \equiv \int_{-\infty}^{\infty} {\phi_*}'(x)^2\,dx = \int_0^{a_*}\sqrt{-2F_*(p)}\,dp, \tag{A.13}$$

we find

$$\int_{R-X}^{R+X} \left(\frac{1}{r}w'^2 - \frac{m^2}{r^3}w^2\right)\,dr \approx \frac{T}{R} - \frac{1}{2}m^2(a_*)^2\left(\frac{1}{(R-X)^2} - \frac{1}{R^2}\right). \tag{A.14}$$

We next approximate the right side of (A.11). Because $w(r) \approx 0$ for $r > R$ and $w(r) \approx a_*$ for $r < R$, we have

$$\begin{aligned} -\left[\frac{1}{2}w'^2 - \frac{m^2}{2r^2}w^2 + F(w)\right]\Bigg|_{R-X}^{R+X} &\approx F(a_*) - \frac{1}{2}\frac{m^2}{(R-X)^2}(a_*)^2 \\ &= \frac{1}{2}(\omega_*-\omega)(a_*)^2 - \frac{1}{2}\frac{m^2}{(R-X)^2}(a_*)^2, \end{aligned} \tag{A.15}$$

where we have used the facts that $F_*(a_*) = 0$ and $F(w) - F_*(w) = \frac{1}{2}(\omega_* - \omega)w^2$.

Combining (A.14) and (A.15), we obtain the quadratic equation

$$(\omega_* - \omega)R^2 - \frac{2T}{(a_*)^2}R - m^2 = 0 \tag{A.16}$$

for R, which depends only on ω and the nonlinearity f_*. The solution for R is given by

$$R \approx R_{\rm out} = \frac{T + \sqrt{T^2 + (a_*)^4 m^2(\omega_* - \omega)}}{(a_*)^2(\omega_* - \omega)}. \tag{A.17}$$

In a similar way, we may approximate the location R of the inner kink of the nodeless wave profile with $m \geq 2$ for $\omega \approx \omega_*$. We find

$$R \approx R_{\rm in} = \frac{-T + \sqrt{T^2 + (a_*)^4 m^2(\omega_* - \omega)}}{(a_*)^2(\omega_* - \omega)}. \tag{A.18}$$

Note that

$$R_{\rm out} - R_{\rm in} = \frac{2T}{(a_*)^2(\omega_* - \omega)}, \tag{A.19}$$

independent of m. For fixed $m \geq 2$ we have

$$R_{\rm in} \to \frac{(a_*)^2 m^2}{2T} \quad \text{and} \quad R_{\rm out} \to \infty \tag{A.20}$$

as ω approaches ω_* from below.

As an example, we consider the cubic-quintic nonlinearity $f(s) = -\omega s + s^3 - s^5$. We have $F(s) = -\frac{1}{2}\omega s^2 + \frac{1}{4}s^4 - \frac{1}{6}s^6$, $\omega_* = \frac{3}{16}$, $a_* = \sqrt{3}/2$, and

$$T = \int_0^{a_*} \sqrt{-2F_*(p)}\; dp = \int_0^{\sqrt{3}/2} \sqrt{\tfrac{1}{3}p^6 - \tfrac{1}{2}p^4 + \tfrac{3}{16}p^2}\; dp = \frac{3\sqrt{3}}{64}. \tag{A.21}$$

Thus we obtain

$$R_{\rm out} = \frac{\sqrt{3} + \sqrt{3 + 256\,(3/16 - \omega)\,m^2}}{16\,(3/16 - \omega)}, \tag{A.22}$$

$$R_{\rm in} = \frac{-\sqrt{3} + \sqrt{3 + 256\,(3/16 - \omega)\,m^2}}{16\,(3/16 - \omega)}, \tag{A.23}$$

which agrees well with the kink locations for the numerically computed wave profiles. E.g., for $m = 3$, $\omega = 0.18$ we get $R_{\rm out} \approx 52$, $R_{\rm in} \approx 23$ In the limit $\omega \to \omega_*$ note that $R_{\rm in} \to 8m^2/\sqrt{3}$.

B Zero modes

Solitary waves are not stable in the ordinary sense that the solution to the evolution equation with perturbed initial data differs little from the unperturbed solution for all time. This can be seen by considering, for example, two solitary waves with slightly different velocities whose initial data are approximately equal but which later drift apart. Instead, solitary-wave stability is defined in terms of the difference between perturbed and unperturbed solutions modulo symmetries of the evolution equation. For instance, the two solitary waves just discussed do remain close modulo spatial translation.

Invariance of an evolution equation under symmetries gives rise to an eigenvalue-zero eigenspace for the generator of time evolution for the equation linearized about a solution. Linear instability due to generalized eigenfunctions in such a space need not correspond to a real instability, but rather to "drift" that can be cancelled by a symmetry transformation. On the other hand, an imaginary eigenvalue with a generalized eigenfunction (of index larger than 1) that does not correspond to a symmetry operation would suggest instability.

In this section we make use of symmetries to enumerate the zero modes of (1.1), obtaining generalized eigenfunctions of the operator A corresponding to eigenvalue $\lambda = 0$. We identify the same number of zero modes that we find numerically.

Given a family u_τ of solutions to (1.1) with smooth dependence on parameter τ, we can differentiate the identity

$$-i\partial_t u_\tau - \Delta u_\tau = g(u_\tau) \tag{B.1}$$

with respect to τ to obtain a solution $\tilde{u}$ to the corresponding equation linearized about u_0:

$$-i\partial_t \tilde{u} - \Delta \tilde{u} = \alpha(|u_0|)\,\tilde{u} + \beta(|u_0|)\frac{u_0}{\bar{u}_0}\bar{\tilde{u}} \tag{B.2}$$

where

$$\tilde{u} \equiv \partial_\tau u_\tau|_{\tau=0}\,. \tag{B.3}$$

We apply this procedure to various one-parameter families of solutions, each having $u_0 = e^{i\omega\,t}v_0(x) = e^{i\omega\,t}e^{i\,m\theta}w(r)$. With $\tilde{v}$ given by $\tilde{u} = e^{i\omega\,t}\tilde{v}$, equation (B.2) becomes

$$\partial_t \tilde{v} = B\tilde{v} \tag{B.4}$$

where B is the real-linear operator given by

$$Bv \equiv i\left((\Delta + \alpha(w) - \sigma^2)\,v + \beta(w)e^{2i\,m\theta}\,\bar{v}\right). \tag{B.5}$$

We note that (B.4) is equivalent to equation (3.4) and that B is the single-component form of the operator A. (Because we are considering the real eigenvalue $\lambda = 0$, in this section we prefer not to work with the two-component form and subsequent complexification.)

- Invariance of NLS under phase changes:

  We define $u_\tau \equiv e^{i\tau}u_0$. Because $g(e^{i\tau}u_0) = e^{i\tau}g(u_0)$ and u_0 is a solution of (1.1), u_τ is a solution for all real τ. For this family, $\tilde{u} = iu_0$ and $\tilde{v} = iv_0$. Since $\tilde{v}$ is time-independent, we see from (B.4) that $\tilde{v}$ is an eigenfunction of B with eigenvalue zero. The corresponding eigenfunction $\mathbf{\Psi} = (\mathrm{Re}\,\tilde{v}, \mathrm{Im}\,\tilde{v})$ of A lies in the $j = 0$ subspace, according to (3.9), (3.13), and (3.14).

- Invariance of NLS under rotation:

  We set $u_\tau \equiv R_\tau u_0$, where R_τ is the coordinate transformation that rotates u_0 by angle τ. Thus $u_\tau = e^{i\omega\,t}e^{i\,m(\theta-\tau)}w(r)$, whence $\tilde{u} = -imu_0$ and $\tilde{v} = -imv_0$. This eigenfunction $\tilde{v}$ of B is a real constant multiple of that induced by invariance under phase change.

- Invariance of NLS under time translation:

  We set $u_\tau(x,t) \equiv u_0(x, t-\tau)$. Then $\tilde{u} = -i\omega u_0$ and $\tilde{v} = -i\omega v_0$. This eigenfunction $\tilde{v}$ of B is a real constant multiple of those induced by invariance under phase change and rotations.

- Invariance of NLS under spatial translation:

  Writing (x, y) for the components of the spatial coordinate vector, we begin by setting $u_\tau(x,y,t) \equiv u_0(x-\tau, y, t)$. Then $\tilde{u} = \partial_x u_0$ and $\tilde{v} = \partial_x v_0$. Since $\tilde{v}$ is time-independent, we see from (B.4) that $\tilde{v}$ is an eigenfunction of B with eigenvalue zero. By explicit computation, we see that according to (3.9), (3.13), and (3.14), the corresponding eigenfunction $\mathbf{\Psi}$ of A has components in the $j = 1$ and $j = -1$ subspaces.

  In a similar way, setting $u_\tau(x,y,t) \equiv u_0(x, y-\tau, t)$ yields the eigenfunction $\tilde{v} = \partial_y v_0$ of the operator B with eigenvalue zero, and the corresponding eigenfunction of A has components in the $j = 1$ and $j = -1$ subspaces. It is straightforward to check that these two eigenfunctions resulting from translations along the x and y axes are linearly independent.

- Invariance of NLS under change of standing-wave frequency:

  As mentioned in Section 2, localized standing-wave solutions $u_0 = e^{i\omega\,t}e^{i\,m\theta}w(r)$ of (1.1) exist for a range of frequencies ω. The radial profile $w(r)$ depends on ω through the differential equation (1.4), in which $f(w) = g(w) - \omega w$. Consequently, v_0 as well as u_0 is parametrized by ω. Differentiating with respect to parameter ω, we have

  $$\tilde{u} = itu_0 + e^{i\omega\,t}\partial_\omega v_0, \quad \tilde{v} = itv_0 + \partial_\omega v_0. \tag{B.6}$$

  Equation (B.4) thus gives $B\tilde{v} = iv_0$. Since we established earlier that $B(iv_0) = 0$, we see that $B\,(\partial_\omega v_0) = iv_0$. Thus (again since $B(iv_0) = 0$),

  $$B^2\,(\partial_\omega v_0) = 0. \tag{B.7}$$

Table 2: Zero modes

Transformation	$\|j\|$	Index	Generalized eigenfunction
Phase, rotation, time translation	0	1	iv_0
Standing-wave frequency change	0	2	$\partial_\omega v_0$
Space translation in x direction	1	1	$\partial_x v_0$
Space translation in y direction	1	1	$\partial_y v_0$
Boost in x direction	1	2	ixv_0
Boost in y direction	1	2	iyv_0

That is, $\partial_\omega v_0$ is a generalized eigenfunction of B of index 2 corresponding to eigenvalue zero. Because

$$\partial_\omega v_0 = e^{i\,m\theta}\partial_\omega w(r), \tag{B.8}$$

the angular dependence of the generalized eigenfunction $\partial_\omega v_0$ is identical to that generated by invariance under phase changes, and as a result the corresponding generalized eigenfunction Ψ of A lies in the $j = 0$ subspace.

- Invariance of NLS under velocity boost:

  Let $c \in \mathbb{R}^2$ be a constant vector. If $u(x,t)$ is a solution to (1.1), then so is the function

$$U_c(x,t) \equiv \exp\left\{ i\left(\frac{1}{2}c\cdot x - \frac{1}{4}\,|c|^2\, t\right)\right\}\; u(x - c\,t,\; t). \tag{B.9}$$

  Again writing (x,y) for the components of the spatial coordinate vector, we first let u_τ be the standing wave u_0 boosted with speed τ in the x coordinate direction (that is, $c = (\tau, 0)$):

$$u_\tau(x,y,t) \equiv \exp\left\{ i\left(\frac{1}{2}\tau\, x - \frac{1}{4}\tau^2 t\right)\right\}\; u_0(x - \tau\, t,\; y,\; t). \tag{B.10}$$

  Then $\tilde{u} = \frac{i}{2}x\, u_0 - t\partial_x u_0$ and $\tilde{v} = \frac{i}{2}x\, v_0 - t\partial_x v_0$. Equation (B.4) thus gives $B\tilde{v} = -\partial_x v_0$. Since we established earlier that $B\,(\partial_x v_0) = 0$, we see that $B(ixv_0) = -2\partial_x v_0$. Therefore (again since $B\,(\partial_x v_0) = 0$),

$$B^2\,(ixv_0) = 0. \tag{B.11}$$

  That is, ixv_0 is a generalized eigenfunction of B of index 2 corresponding to eigenvalue zero. By explicit computation, we see that the corresponding eigenfunction $\mathbf{\Psi}$ of A has components in the $j = 1$ and $j = -1$ subspaces.

  In a similar way, letting u_τ be the standing wave u_0 boosted with speed τ in the y coordinate direction (that is, $c = (0, \tau)$), we find that iyv_0 is a generalized eigenfunction of B of index 2 corresponding to eigenvalue zero, and the corresponding eigenfunction of A has components in the $j = 1$ and $j = -1$ subspaces. The two generalized eigenfunctions ixv_0 and iyv_0 resulting from velocity boosts in the x and y directions are linearly independent.

We have thus found two $j = 0$ generalized eigenfunctions, and four $|j| = 1$ generalized eigenfunctions, for eigenvalue $\lambda = 0$, as summarized in Table 2.

To establish that these Jordan chains of generalized eigenfunctions do in fact terminate with index 2 in the general case, we make use of the following observation.

Lemma B.1 *Suppose $A = JL$ where L is self-adjoint and $J^* = J^{-1} = -J$. Suppose Ψ_K is a generalized eigenfunction of A with index K corresponding to eigenvalue zero. If there exists Φ in the*

domain of A such that $A\Phi = \Psi_K$, then $\langle \Psi_j \, | J\Psi_{K+1-j} \rangle = 0$ for $j = 1, \ldots, K$, where $\Psi_j \equiv A^{K-j}\Psi_K$.

Proof From the definition of Ψ_j it follows that $A\Psi_j = \Psi_{j-1}$ and $A^j\Psi_j = 0$ but $A^{j-1}\Psi_j \neq 0$. Thus Ψ_j is a generalized eigenfunction of A with index j.

Define $\Psi_j^* \equiv J\Psi_j$. From the assumed form for A we then have

$$A^*\Psi_j^* = -JA\Psi_j = -J\Psi_{j-1} = -\Psi_{j-1}^*. \tag{B.12}$$

It follows that

$$(A^*)^j\Psi_j^* = (-1)^j JA\Psi_1 = 0. \tag{B.13}$$

Thus, for $1 \leq j \leq K$, we have

$$\begin{aligned} \langle \Psi_j \, | J\Psi_{K+1-j} \rangle &= -\left\langle \Psi_j^* \, | \Psi_{K+1-j} \right\rangle = -\left\langle \Psi_j^* \, | A^{j-1}\Psi_K \right\rangle \\ &= -\left\langle \Psi_j^* \, | A^{j-1}A\Phi \right\rangle = -\left\langle \Psi_j^* \, | A^j\Phi \right\rangle \\ &= -\left\langle (A^*)^j\Psi_j^* \, | \Phi \right\rangle = 0, \end{aligned} \tag{B.14}$$

as asserted. □

We now apply this observation to our index-2 generalized eigenfunctions. Consider first the generalized eigenfunction $\psi_2 = ixv_0$ of B arising from velocity boost in the x direction. Then $\psi_1 \equiv B\psi_2 = -2\partial_x v_0$ and we have

$$\langle \Psi_1 \, | J\Psi_2 \rangle = \mathrm{Re} \, \langle \psi_1 \, | i \, \psi_2 \rangle = \mathrm{Re} \, \langle -2\partial_x v_0 \, | i \, ixv_0 \rangle = - \left\| v_0 \right\|^2 \neq 0. \tag{B.15}$$

Thus there is no generalized eigenfunction in this Jordan chain with index 3 (or higher). Similarly, analyzing the index-2 generalized eigenfunction $\psi_2 = iyv_0$ of B arising from velocity boost in the y direction, we find that there is no generalized eigenfunction in this chain with higher index.

We next consider the index-2 generalized eigenfunction $\psi_2 = \partial_\omega v_0$ of B arising from change of standing-wave frequency, which lies in the $j = 0$ subspace. We set $\psi_1 \equiv B\psi_2 = iv_0$, and we find

$$\langle \Psi_1 \, | J\Psi_2 \rangle = \mathrm{Re} \, \langle \psi_1 \, | i \, \psi_2 \rangle = \mathrm{Re} \, \langle iv_0 \, | i \, \partial_\omega v_0 \rangle = \tfrac{1}{2}\partial_\omega \left\| v_0 \right\|^2. \tag{B.16}$$

Generically, we expect the quantity $\partial_\omega \left\| v_0 \right\|^2$ to be nonzero, hence that $\psi_2 = \partial_\omega v_0$ is the highest-index generalized eigenfunction in this Jordan chain. Our numerical studies confirm this expectation for nonlinearities other than pure cubic.

The six-dimensional eigenspace for eigenvalue zero summarized in the table is in agreement with our numerical observations. For nonlinearities other than pure cubic, we find numerically that the eigenvalue zero has multiplicity two in each of the $j = 0$, $j = 1$, and $j = -1$ subspaces.

In contrast, in the special case of a purely cubic nonlinearity $g(u) = \gamma|u|^2u$ in two spatial dimensions, the norm $\left\| v_0 \right\|^2$ is independent of ω. To see this, we note that the function $\tilde{v}_0$ defined by $v_0(x) = \sqrt{\omega/\gamma}\, \tilde{v}_0(\sqrt{\omega}\, x)$ satisfies the ω-independent equation $\Delta\tilde{v}_0 - \tilde{v}_0 + |\tilde{v}_0|^2\tilde{v}_0 = 0$. It is straightforward to compute that, in N spatial dimensions, $\left\| v_0 \right\|^2 = \frac{1}{\gamma}\omega^{(2-N)/2} \left\| \tilde{v}_0 \right\|^2$. Thus, for the pure-cubic nonlinearity, in $N = 2$ spatial dimensions, the index-2 generalized eigenfunction does not necessarily terminate the Jordan chain in the $j = 0$ subspace, and in fact generalized eigenfunctions with indices 3 and 4 are present in this special case.

The structure of the generalized null spaces of A in the case of (1.1) with pure-power nonlinearities is established in Appendix B of the paper [33]. The index-3 generalized eigenfunction $\psi_3 = ir^2v_0$ of B arises from the invariance of cubic NLS in two spatial dimensions under the Talanov lens transformation. An index-4 generalized eigenfunction ψ_4 has the form $\psi_4 = \xi(r)e^{im\theta}$, where ξ is the bounded solution to the ordinary differential equation $L_3\xi = r^2w_0$, where

$$L_3 = \frac{\partial^2}{\partial r^2} + \frac{1}{r}\frac{\partial}{\partial r} - \frac{m^2}{r^2} - \omega + 3\gamma w_0^2.$$

There are no generalized eigenfunctions with higher index. Our numerical observations in the pure cubic case show that eigenvalue zero has multiplicity four in the $j = 0$ subspace, in agreement with this analysis.

C Two proofs

It remains to prove two technical results needed to characterize eigenvalues.

C.1 Proof of Lemma 4.1

To prove Lemma 4.1, we will transform the system (4.6)

$$\boldsymbol{y}' = \boldsymbol{B}(r, j, \lambda)\boldsymbol{y}$$

to an equivalent system of the form $\boldsymbol{\zeta}' = (\overset{\circ}{\boldsymbol{C}} + \tilde{\boldsymbol{C}})\boldsymbol{\zeta}$ where $\overset{\circ}{\boldsymbol{C}}$ is constant and $\tilde{\boldsymbol{C}}$ is integrable, then make use of facts concerning asymptotic behavior of solutions to such systems. To do so, we make the change of variables $\zeta_\pm(x) = h(r)y_\pm(r)$, where $x = x(r)$ and $h(r)$ are smooth monotonic functions such that

$$x(r) = \begin{cases} \ln r & \text{for } r < \frac{1}{2}, \\ r & \text{for } r > 2, \end{cases} \qquad h(r) = \begin{cases} 1 & \text{for } r < \frac{1}{2}, \\ \sqrt{r} & \text{for } r > 2. \end{cases} \tag{C.1}$$

With this change of variables, system (4.6) is equivalent to

$$\boldsymbol{\zeta}' = \boldsymbol{C}(x)\boldsymbol{\zeta}, \tag{C.2}$$

where

$$\boldsymbol{\zeta}(x) = \begin{pmatrix} \zeta_+ \\ \zeta_+' \\ \zeta_- \\ \zeta_-' \end{pmatrix} = M(r)\boldsymbol{y}(r), \quad M(r) = \begin{pmatrix} h & 0 & 0 & 0 \\ h'r_x & hr_x & 0 & 0 \\ 0 & 0 & h & 0 \\ 0 & 0 & h'r_x & hr_x \end{pmatrix}, \tag{C.3}$$

and

$$\boldsymbol{C}(x) = r_x(M\boldsymbol{B}M^{-1} + M'M^{-1}). \tag{C.4}$$

Note that

$$\begin{pmatrix} h & 0 \\ h'r_x & hr_x \end{pmatrix} = \begin{pmatrix} 1 & 0 \\ 0 & r \end{pmatrix}, \quad \text{resp.} \quad \begin{pmatrix} \sqrt{r} & 0 \\ \frac{1}{2\sqrt{r}} & \sqrt{r} \end{pmatrix}, \tag{C.5}$$

for $r < \frac{1}{2}$ and $r > 2$.

We can write $\boldsymbol{C}(x) = \overset{\circ}{\boldsymbol{C}} + \tilde{\boldsymbol{C}}(x)$, where

$$\overset{\circ}{\boldsymbol{C}} = \begin{pmatrix} 0 & 1 & 0 & 0 \\ (j+m)^2 & 0 & 0 & 0 \\ 0 & 0 & 0 & 1 \\ 0 & 0 & (j-m)^2 & 0 \end{pmatrix}, \quad \text{resp.} \quad \begin{pmatrix} 0 & 1 & 0 & 0 \\ k_+^2 & 0 & 0 & 0 \\ 0 & 0 & 0 & 1 \\ 0 & 0 & k_-^2 & 0 \end{pmatrix}, \tag{C.6}$$

for $x < -\ln 2$ and $x > 2$, and where the entries of $\tilde{\boldsymbol{C}}(x)$ are $O(1/x^2)$ as $x \to \infty$ and $O(e^{2x})$ as $x \to -\infty$, so that $\tilde{\boldsymbol{C}}(x)$ (but not $x\tilde{\boldsymbol{C}}(x)$) is absolutely integrable on $\mathbb{R}$.

We discuss the asymptotic behavior of solutions as $|x| \to \infty$ in the intervals $(2, \infty)$ and $(-\infty, -\ln 2)$ separately. We note first that because k_+ and k_- are nonzero, the matrix $\overset{\circ}{\boldsymbol{C}}$ is constant and diagonalizable on $(2, \infty)$, with eigenvalues k_+, k_-, $-k_+$, and $-k_-$. The system $\boldsymbol{\zeta}' = \overset{\circ}{\boldsymbol{C}}\,\boldsymbol{\zeta}$ on $(2, \infty)$ has the fundamental set of solutions

$$e^{k_+x}\begin{pmatrix} 1 \\ k_+ \\ 0 \\ 0 \end{pmatrix}, \quad e^{k_-x}\begin{pmatrix} 0 \\ 0 \\ 1 \\ k_- \end{pmatrix}, \quad e^{-k_+x}\begin{pmatrix} 1 \\ -k_+ \\ 0 \\ 0 \end{pmatrix}, \quad e^{-k_-x}\begin{pmatrix} 0 \\ 0 \\ 1 \\ -k_- \end{pmatrix}. \tag{C.7}$$

It follows from Theorem IV.1 of [7] that for each member of this fundamental set, there exists a solution $\boldsymbol{\zeta}$ of (C.2) that is asymptotic to it as $x \to \infty$. Undoing the change of variables on the interval $(2, \infty)$, we see that system (4.6) has corresponding solutions respectively asymptotic to

$$\frac{e^{k_+ r}}{\sqrt{r}} \begin{pmatrix} 1 \\ k_+ \\ 0 \\ 0 \end{pmatrix}, \quad \frac{e^{k_- r}}{\sqrt{r}} \begin{pmatrix} 0 \\ 0 \\ 1 \\ k_- \end{pmatrix}, \quad \frac{e^{-k_+ r}}{\sqrt{r}} \begin{pmatrix} 1 \\ -k_+ \\ 0 \\ 0 \end{pmatrix}, \quad \frac{e^{-k_- r}}{\sqrt{r}} \begin{pmatrix} 0 \\ 0 \\ 1 \\ -k_- \end{pmatrix} \tag{C.8}$$

as $r \to \infty$. Since the modified Bessel functions I_ν and K_ν have the asymptotic forms

$$I_\nu(z) = \frac{1}{\sqrt{2\pi z}}\, e^z \left(1 + O\left(\frac{1}{|z|}\right)\right), \quad K_\nu(z) = \sqrt{\frac{\pi}{2z}}\, e^{-z} \left(1 + O\left(\frac{1}{|z|}\right)\right) \tag{C.9}$$

as $|z| \to \infty$ in the right half complex plane, we see that the system (4.6) has solutions asymptotic to $\overset{\circ}{\boldsymbol{y}}_i$ as $r \to \infty$, for each $i = 1, \ldots, 4$ as claimed.

To analyze the asymptotic behavior of solutions as $r \to 0^+$, we first suppose that both $j + m$ and $j - m$ are nonzero. Then the matrix $\overset{\circ}{\boldsymbol{C}}$ is constant and diagonalizable on $(-\infty, -\ln 2)$, with eigenvalues $|j + m|$, $|j - m|$, $-|j + m|$, and $-|j - m|$. The system $\boldsymbol{\zeta}' = \overset{\circ}{\boldsymbol{C}}\, \boldsymbol{\zeta}$ on $(-\infty, -\ln 2)$ has the fundamental set of solutions

$$e^{|j+m|x} \begin{pmatrix} 1 \\ |j+m| \\ 0 \\ 0 \end{pmatrix}, \; e^{|j-m|x} \begin{pmatrix} 0 \\ 0 \\ 1 \\ |j-m| \end{pmatrix}, \; e^{-|j+m|x} \begin{pmatrix} 1 \\ -|j+m| \\ 0 \\ 0 \end{pmatrix}, \; e^{-|j-m|x} \begin{pmatrix} 0 \\ 0 \\ 1 \\ -|j-m| \end{pmatrix}. \tag{C.10}$$

It follows as before that for each of these, there is a solution $\boldsymbol{\zeta}$ of (C.2) asymptotic to it as $x \to -\infty$. Undoing the change of variables on the interval $(-\infty, -\ln 2)$, we see that the system (4.6) has corresponding solutions respectively asymptotic to

$$r^{|j+m|} \begin{pmatrix} 1 \\ \frac{|j+m|}{r} \\ 0 \\ 0 \end{pmatrix}, \; r^{|j-m|} \begin{pmatrix} 0 \\ 0 \\ 1 \\ \frac{|j-m|}{r} \end{pmatrix}, \; r^{-|j+m|} \begin{pmatrix} 1 \\ -\frac{|j+m|}{r} \\ 0 \\ 0 \end{pmatrix}, \; r^{-|j-m|} \begin{pmatrix} 0 \\ 0 \\ 1 \\ -\frac{|j-m|}{r} \end{pmatrix} \tag{C.11}$$

as $r \to 0^+$. Since for $\nu > 0$ the modified Bessel functions I_ν and K_ν have the asymptotic forms

$$I_\nu(z) = \frac{(\frac{1}{2}z)^\nu}{\Gamma(\nu + 1)}(1 + O(|z|)), \quad K_\nu(z) = \frac{\frac{1}{2}\Gamma(\nu)}{(\frac{1}{2}z)^\nu}(1 + O(|z|)) \tag{C.12}$$

as $z \to 0$, we see that the system (4.6) has a solution asymptotic to $\overset{\circ}{\boldsymbol{y}}_i$ as $r \to 0$ for each $i = 1, \ldots, 4$, as claimed.

If either $j + m = 0$ or $j - m = 0$, then on $(-\infty, -\ln 2)$ the matrix $\overset{\circ}{\boldsymbol{C}}$ is constant and has Jordan canonical form with a block of order 2 corresponding to the eigenvalue zero. Suppose for definiteness that $j = m > 0$. Then on $(-\infty, -\ln 2)$ we have

$$\overset{\circ}{\boldsymbol{C}} = \begin{pmatrix} 0 & 1 & 0 & 0 \\ 4m^2 & 0 & 0 & 0 \\ 0 & 0 & 0 & 1 \\ 0 & 0 & 0 & 0 \end{pmatrix}, \tag{C.13}$$

and the system $\boldsymbol{\zeta}' = \overset{\circ}{\boldsymbol{C}}\, \boldsymbol{\zeta}$ has the fundamental set of solutions

$$e^{2mx} \begin{pmatrix} 1 \\ 2m \\ 0 \\ 0 \end{pmatrix}, \quad \begin{pmatrix} 0 \\ 0 \\ 1 \\ 0 \end{pmatrix}, \quad e^{-2mx} \begin{pmatrix} 1 \\ -2m \\ 0 \\ 0 \end{pmatrix}, \quad \begin{pmatrix} 0 \\ 0 \\ x \\ 1 \end{pmatrix}. \tag{C.14}$$

Since the entries of the matrix $\tilde{\boldsymbol{C}}(x)$ decay exponentially to zero as $x \to -\infty$, $x\tilde{\boldsymbol{C}}(x)$ is absolutely integrable on $(-\infty, -\ln 2)$, and we may apply Theorem IV.4 of [7] to establish that for each member of this set of solutions, there exists a solution $\boldsymbol{\zeta}$ of (C.2) that is asymptotic to it as $x \to -\infty$. Undoing the change of variables on the interval $(-\infty, -\ln 2)$, we see that the system (4.6) has corresponding solutions respectively asymptotic to

$$r^{2m}\begin{pmatrix}1\\2m/r\\0\\0\end{pmatrix}, \quad \begin{pmatrix}0\\0\\1\\0\end{pmatrix}, \quad r^{-2m}\begin{pmatrix}1\\-2m/r\\0\\0\end{pmatrix}, \quad \begin{pmatrix}0\\0\\\ln r\\1/r\end{pmatrix} \tag{C.15}$$

as $r \to 0$. Since $I_0(z) \sim 1$ and $K_0(z) \sim -\ln z$ as $z \to 0$, we see that the system (4.6) in this case again has a solution asymptotic to $\overset{\circ}{\boldsymbol{y}}_i$ as $r \to 0$ for each $i = 1, \ldots, 4$. This finishes the proof of the Lemma. □

C.2 Proof of Proposition 4.6

It is evident that for any given $\lambda \in \mathbb{C}_\sigma$, the exterior systems associated with (4.6) and its adjoint (4.13) have the respective solutions $\hat{\boldsymbol{y}} = \boldsymbol{y}_1^{(0)} \wedge \boldsymbol{y}_2^{(0)}$ and $\hat{\boldsymbol{z}} = \boldsymbol{z}_1^{(\infty)} \wedge \boldsymbol{z}_2^{(\infty)}$ with the desired asymptotic behavior, since

$$\begin{array}{rcll} \boldsymbol{y}_1^{(0)} \wedge \boldsymbol{y}_2^{(0)} & \sim & \overset{\circ}{\boldsymbol{y}}_1 \wedge \overset{\circ}{\boldsymbol{y}}_2 & \text{as } r \to 0^+, \\ \boldsymbol{z}_1^{(\infty)} \wedge \boldsymbol{z}_2^{(\infty)} & \sim & \overset{\circ}{\boldsymbol{z}}_1 \wedge \overset{\circ}{\boldsymbol{z}}_2 & \text{as } r \to \infty. \end{array} \tag{C.16}$$

It remains to establish the uniqueness and analyticity of these solutions. Our plan is to transform the associated exterior systems to corresponding systems on the whole line by changing variables as in the proof of Lemma 4.1. Under this transformation, the quantities $\boldsymbol{y}_1^{(0)} \wedge \boldsymbol{y}_2^{(0)}$ and $\boldsymbol{z}_1^{(\infty)} \wedge \boldsymbol{z}_2^{(\infty)}$ map to solutions having asymptotic normalizations that enjoy a maximal rate of decay property. Uniqueness and analyticity of these solutions is a consequence of the theory of [26].

Let $x(r)$, $h(r)$, and $M(r)$ be as in (C.1) and (C.3). Suppose $\hat{\boldsymbol{y}}(r)$ is a solution of the exterior system

$$\hat{\boldsymbol{y}}' = \boldsymbol{B}_\wedge(r)\hat{\boldsymbol{y}} \tag{C.17}$$

associated with (4.6). Then $\hat{\boldsymbol{y}}$ may be written as a linear combination of solutions of the form $\boldsymbol{y} \wedge \tilde{\boldsymbol{y}}$ where $\boldsymbol{y}$ and $\tilde{\boldsymbol{y}}$ are solutions of (4.6). (Do this first for initial data, then solve the initial-value problem.) Given such solutions, then $\boldsymbol{\zeta}(x) := M(r)\boldsymbol{y}(r)$ and $\tilde{\boldsymbol{\zeta}}(x) := M(r)\tilde{\boldsymbol{y}}(r)$ are solutions of (C.2), and $\hat{\boldsymbol{\zeta}} := \boldsymbol{\zeta} \wedge \tilde{\boldsymbol{\zeta}}$ is a solution of the exterior system

$$\hat{\boldsymbol{\zeta}}' = \boldsymbol{C}_\wedge(x)\hat{\boldsymbol{\zeta}} \tag{C.18}$$

associated with (C.2). Note that

$$\boldsymbol{\zeta} \wedge \tilde{\boldsymbol{\zeta}} = (M\boldsymbol{y}) \wedge (M\tilde{\boldsymbol{y}}) = \hat{M}(\boldsymbol{y} \wedge \tilde{\boldsymbol{y}}),$$

where the 6×6 matrix $\hat{M}$ has columns determined by $\hat{M}(\boldsymbol{e}_j \wedge \boldsymbol{e}_k) = (M\boldsymbol{e}_j) \wedge (M\boldsymbol{e}_k)$. It follows that if we let $\hat{\boldsymbol{\zeta}}(x) = \hat{M}(r)\hat{\boldsymbol{y}}(r)$, then $\hat{\boldsymbol{\zeta}}$ is a solution of (C.18). Similarly, the converse holds: if $\hat{\boldsymbol{\zeta}}$ is a solution of (C.18) and $\hat{\boldsymbol{y}}(r) = \hat{M}(r)^{-1}\hat{\boldsymbol{\zeta}}(x)$, then $\hat{\boldsymbol{y}}$ is a solution of (C.17). (Note that if $N = M^{-1}$, then $\hat{N}\hat{M}(\boldsymbol{y} \wedge \tilde{\boldsymbol{y}}) = \boldsymbol{y} \wedge \tilde{\boldsymbol{y}}$ for all 4-vectors $\boldsymbol{y}$ and $\tilde{\boldsymbol{y}}$, hence $\hat{N} = \hat{M}^{-1}$.)

We transform the adjoint exterior system in similar fashion. Suppose $\hat{\boldsymbol{\eta}}(x) = \hat{\boldsymbol{z}}(r)\hat{M}(r)^{-1}$. Then $\hat{\boldsymbol{z}}$ is a solution of the exterior system

$$\hat{\boldsymbol{z}}' = -\hat{\boldsymbol{z}}\boldsymbol{B}_\wedge(r) \tag{C.19}$$

associated with (4.13) if and only if $\hat{\boldsymbol{\eta}}$ is a solution of the exterior system

$$\hat{\boldsymbol{\eta}}' = -\hat{\boldsymbol{\eta}}\boldsymbol{C}_\wedge(x) \tag{C.20}$$

associated with the equation adjoint to (C.2).

Let us now study solutions of (C.20) that correspond to solutions of (C.19) with the asymptotic behavior in (C.16). Using the asymptotic relations established in Lemma 4.4, the definitions (4.15) and (4.4), and the asymptotics in (C.9), we determine that

$$(\boldsymbol{z}_1^{(\infty)} \wedge \boldsymbol{z}_2^{(\infty)})\hat{M}^{-1} \sim \left(\overset{\circ}{\boldsymbol{z}}_1 M^{-1}\right) \wedge \left(\overset{\circ}{\boldsymbol{z}}_2 M^{-1}\right) \sim \exp(-\hat{\mu}^{(\infty)}x)\hat{\boldsymbol{w}}^{(\infty)} \tag{C.21}$$

as $x \to \infty$, where $\hat{\mu}^{(\infty)} = k_+ + k_-$ is an eigenvalue of $\overset{\circ}{\boldsymbol{C}}_\wedge$ for $x > 2$, and $\hat{\boldsymbol{w}}^{(\infty)}$ is the particular associated left eigenvector

$$\hat{\boldsymbol{w}}^{(\infty)} = \frac{\pi}{2\sqrt{k_+k_-}}(k_+, 1, 0, 0) \wedge (0, 0, k_-, 1). \tag{C.22}$$

Since k_+ and k_- have positive real parts for $\lambda \in \mathbb{C}_\sigma$, it follows that $\hat{\mu}^{(\infty)}$ is a simple eigenvalue, and $\hat{\mu}^{(\infty)}$ is the *unique* eigenvalue of largest real part. For $\lambda \in \mathbb{C}_\sigma$, it is clear that $\hat{\mu}^{(\infty)}$ and $\hat{\boldsymbol{w}}^{(\infty)}$ are analytic and the latter is nonvanishing.

Since $\tilde{\boldsymbol{C}}_\wedge(x) = \boldsymbol{C}_\wedge(x) - \overset{\circ}{\boldsymbol{C}}_\wedge$ is integrable on $\mathbb{R}$, we may now invoke the theory of [26]. Proposition 1.2 of [26] asserts (after space reversal) that (C.20) has a unique solution $\hat{\boldsymbol{\eta}}^{(\infty)}(x, \lambda)$ satisfying

$$\exp(\hat{\mu}^{(\infty)}x)\hat{\boldsymbol{\eta}}^{(\infty)}(x, \lambda) \to \hat{\boldsymbol{w}}^{(\infty)} \quad \text{as } x \to \infty, \tag{C.23}$$

and this solution is globally analytic in λ for $\lambda \in \mathbb{C}_\sigma$. It follows that $\hat{\boldsymbol{z}}^{(\infty)}(r, \lambda) := \hat{\boldsymbol{\eta}}^{(\infty)}(x, \lambda)\hat{M}(r)$ yields the unique solution of (C.19) having the asymptotic behavior asserted in Proposition 4.6, and that $\hat{\boldsymbol{z}}^{(\infty)}$ is analytic in λ for $\lambda \in \mathbb{C}_\sigma$.

The treatment of (C.17) is similar, at least in the case when $|j+m|$ and $|j-m|$ are both nonzero, which we consider first. As $x \to -\infty$ we have

$$\hat{M}(\boldsymbol{y}_1^{(0)} \wedge \boldsymbol{y}_2^{(0)}) \sim \left(M\,\overset{\circ}{\boldsymbol{y}}_1\right) \wedge \left(M\,\overset{\circ}{\boldsymbol{y}}_2\right) \sim \exp(\hat{\mu}^{(-\infty)}x)\hat{\boldsymbol{v}}^{(-\infty)} \tag{C.24}$$

where $\hat{\mu}^{(-\infty)} = |j+m| + |j-m|$ is an eigenvalue of $\overset{\circ}{\boldsymbol{C}}_\wedge$ for $x < -\ln 2$, and $\hat{\boldsymbol{v}}^{(-\infty)}$ is the particular associated right eigenvector

$$\hat{\boldsymbol{v}}^{(-\infty)} = \frac{(\frac{1}{2}k_+)^{|j+m|}(\frac{1}{2}k_-)^{|j-m|}}{\Gamma(|j+m|)\Gamma(|j-m|)} \begin{pmatrix} 1 \\ |j+m| \\ 0 \\ 0 \end{pmatrix} \wedge \begin{pmatrix} 0 \\ 0 \\ 1 \\ |j-m| \end{pmatrix}. \tag{C.25}$$

Clearly $\hat{\mu}^{(-\infty)}$ is independent of λ, and $\hat{\boldsymbol{v}}^{(-\infty)}$ is analytic and nonvanishing in the cut plane $\mathbb{C}_\sigma$. Provided $|j+m|$ and $|j-m|$ are nonzero, $\hat{\mu}^{(-\infty)}$ is simple and is the *unique* eigenvalue of largest real part for $\overset{\circ}{\boldsymbol{C}}_\wedge$ for $x < -\ln 2$. Proposition 1.2 of [26] implies that (C.18) has a unique solution $\hat{\boldsymbol{\zeta}}^{(-\infty)}(x, \lambda)$ satisfying

$$\exp(-\hat{\mu}^{(-\infty)}x)\hat{\boldsymbol{\zeta}}^{(-\infty)}(x, \lambda) \to \hat{\boldsymbol{v}}^{(-\infty)} \quad \text{as } x \to -\infty, \tag{C.26}$$

and this solution is globally analytic for $\lambda \in \mathbb{C}_\sigma$. It follows that $\hat{\boldsymbol{y}}^{(0)} := \hat{M}^{-1}\hat{\boldsymbol{\zeta}}^{(-\infty)}$ is the unique solution of (C.17) having the asymptotic behavior asserted in Proposition 4.6, and that $\hat{\boldsymbol{y}}^{(0)}$ is analytic in λ for $\lambda \in \mathbb{C}_\sigma$.

It remains to consider the case when either $|j+m|$ or $|j-m|$ is zero. For definiteness, suppose $j = m > 0$. We still have (C.24), and $\hat{\mu}^{(-\infty)}$ is the unique eigenvalue of largest real part, but now it

is a double eigenvalue of geometric multiplicity one, with eigenspace spanned by $\hat{\boldsymbol{v}}^{(-\infty)}$. The proof of Proposition 1.2 of [26] must be modified to obtain the uniqueness and analyticity of $\hat{\boldsymbol{\zeta}}^{(-\infty)}$.

This can be done as follows. First, we change variables in (C.18), writing

$$\boldsymbol{v}(x) = \exp(-\hat{\mu}^{(-\infty)}x)\hat{\boldsymbol{\zeta}}(x) \tag{C.27}$$

Let $B = \mathring{\boldsymbol{C}}_\wedge - \hat{\mu}^{(-\infty)}I$ and $R(x,\lambda) = \tilde{\boldsymbol{C}}_\wedge(x)$. Then the first equation in (C.18) is equivalent to

$$\boldsymbol{v}'(x) = (B + R(x,\lambda))\,\boldsymbol{v}.$$

Note that there is a constant $C_1 > 0$ independent of λ such that

$$\|\exp(Bx)\| \le C_1(1+|x|)$$

for all $x \ge 0$. Also, the entries of $R(x,\lambda)$ decay exponentially as $x \to -\infty$, uniformly for λ in any compact subset of $\mathbb{C}_\sigma$. For any compact subset $\Omega_1 \subset \mathbb{C}_\sigma$, there exists x_0 sufficiently negative so that

$$\theta = C_1 \sup_{\lambda\in\Omega_1} \int_{-\infty}^{x_0} (1+|s|)\|R(s,\lambda)\|\,ds < 1.$$

We define an operator $\mathcal{F} = \mathcal{F}(\lambda)$ on the space $C((-\infty,x_0])$ of bounded continuous functions on $(-\infty,x_0]$ by

$$\mathcal{F}\boldsymbol{v}(x) = \int_{-\infty}^{x} e^{(x-s)B}R(s,\lambda)v(s)\,ds.$$

Then it follows that for $\lambda \in \Omega_1$,

$$\sup_{x<x_0} |\mathcal{F}\boldsymbol{v}(x)| \le \theta \sup_{x<x_0} |\boldsymbol{v}(x)|.$$

From here, the proof goes the same as the proof of Proposition 1.2 of [26]. The equation $\boldsymbol{v} = \tilde{\boldsymbol{v}} + \mathcal{F}\boldsymbol{v}$ yields a bicontinuous correspondence between bounded solutions of (C.27) on $(-\infty,x_0]$, and those of $\tilde{\boldsymbol{v}}' = B\tilde{\boldsymbol{v}}$, all of which have the form $\tilde{\boldsymbol{v}}(x) = c\hat{\boldsymbol{v}}^{(-\infty)}$ for some $c \in \mathbb{C}$. The solution we seek has the representation

$$\hat{\boldsymbol{\zeta}}^{(-\infty)}(x) = \exp(\hat{\mu}^{(-\infty)}x)(I-\mathcal{F})^{-1}\hat{\boldsymbol{v}}^{(-\infty)}$$

for $x < x_0$, and is extended by solving (C.18). It is independent of x_0 and is obtained by iterations that are analytic in λ and converge uniformly for $x < x_0$, $\lambda \in \Omega_1$. It follows that $\hat{\boldsymbol{\zeta}}^{(-\infty)}(x)$ is globally analytic for $\lambda \in \mathbb{C}_\sigma$. This finishes the proof of the Proposition. □

Acknowledgements

This material is based upon work supported by the National Science Foundation under Grant Nos. DMS97-04924 and DMS00-72609 and SCREMS grant DMS96-28467. This work was partially supported by University of North Texas Faculty Research Grants and by the University of Maryland Graduate Research Board. The authors thank B. A. Malomed and I. Towers for communicating their work [31] prior to publication.

References

[1] A. L. Afendikov and T. J. Bridges. Instability of the Hocking-Stewartson pulse and its implications for three-dimensional Poiseuille flow. *Proc. Roy. Soc. Lond. A*, 457:257–272, 2001.

[2] J. Alexander, R. Gardner, and C. K. R. T. Jones. A topological invariant arising in the stability analysis of traveling waves. *J. Reine Angew. Math.*, 410:167–212, 1990.

[3] J. Alexander and R. L. Sachs. Linear instability of solitary waves of a Boussinesq-type equation: a computer assisted computation. *Nonlin. World*, 2:471–507, 1995.

[4] C. De Angelis. Self-trapped propagation in the nonlinear cubic-quintic Schrödinger equation — a variational approach. *IEEE J. Quant. Electon.*, 30:818–821, 1994.

[5] M. Axenides, E. Floratos, S. Komineas, and L. Perivolaropoulos. Metastable ringlike semitopological solitons. *Phys. Rev. Lett.*, 86:4459–4462, 2001.

[6] S. Coleman. Q-balls. *Nuclear Phys. B*, 262:263–283, 1985.

[7] W. A. Coppel. *Stability and Asymptotic Behavior of Differential Equations*. D.C. Heath and Co., Boston, 1965.

[8] L.-C. Crasovan, B. A. Malomed, and D. Mihalache. Stable vortex solitons in the two-dimensional Ginzburg-Landau equation. *Phys. Rev. E*, 63:016605, 2000.

[9] A. Desyatnikov, A. Maimistov, and B. Malomed. Three-dimensional spinning solitons in dispersive media with the cubic-quintic nonlinearity. *Phys. Rev. E*, 61(3):3107–3113, 2000.

[10] K. Dimitrevski, E. Reimhult, E. Svensson, A. Öhgren, D. Anderson, A. Berntson, M. Lisak, and M. L. Quiroga-Teixeiro. Analysis of stable self-trapping of laser beams in cubic-quintic nonlinear media. *Phys. Lett. A*, 248:369–376, 1998.

[11] G. Y. Fang, Y. L. Song, Y. X. Wang, X. R. Zhang, S. L. Qu, C. F. Li, L. C. Song, Q. M. Hu, and P. C. Liu. Self focusing-self defocusing transformation in an organometalic fullerene-C_{60} derivative. *Acta Physica Sinica*, 49(8):1499–1502, 2000.

[12] W. J. Firth and D. V. Skryabin. Optical solitons carrying orbital angular momentum. *Phys. Rev. Lett.*, 79:2450–2453, 1997.

[13] M. Grillakis, J. Shatah, and W. Strauss. Stability theory of solitary waves in the presence of symmetry, ii. *J. Func. Anal.*, 74:308–348, 1990.

[14] J. Iaia and H. Warchall. Nonradial solutions of a semilinear elliptic equation in two dimensions. *J. Diff. Eq.*, 119:533–558, 1995.

[15] J. Iaia and H. Warchall. Encapsulated-vortex solutions to equivariant wave equations: Existence. *SIAM J Math Anal*, 30:118–139, 1998.

[16] J. Iaia, H. Warchall, and F. B. Weissler. Localized solutions of sublinear elliptic equations: Loitering at the hilltop. *Rocky Mountain J. Math.*, 27:1131–1157, 1997.

[17] B. L. Lawrence, M. Cha, J. U. Kang, W. Torruellas, G. Stegeman, G. Baker, J. Meth, and S. Etemad. Large purely refractive nonlinear index of single-crystal p-toluene sulfonate (PTS) at 1600 nm. *Electron. Lett.*, 30:447–448, 1994.

[18] B. L. Lawrence, M. Cha, W. E. Torruellas, and G. I. Stegeman. Measurement of the complex nonlinear refractive index of single crystal *p*-toluene sulfonate at 1064 nm. *Appl. Phys. Lett.*, 64(21):2773–2775, 1994.

[19] B. L. Lawrence and G. I. Stegeman. Two-dimensional bright spatial solitons stable over limited intensities and ring formation in polydiacetylene para-toluene sulfonate. *Opt. Lett.*, 23(8):591–593, 1998.

[20] D. Mihalache, D. Mazilu, L.-C. Crasovan, B. A. Malomed, and F. Lederer. Azimuthal instability of spinning spatiotemporal solitons. *Phys. Rev. E*, 62:1505(R), 2000.

[21] D. Mihalache, D. Mazilu, L.-C. Crasovan, B. A. Malomed, and F. Lederer. Three-dimensional spinning solitons in the cubic-quintic nonlinear medium. *Phys. Rev. E*, 61:7142–7145, 2000.

[22] J. Neu. Vortices in complex scalar fields. *Physica D*, 43:385–406, 1990.

[23] P. K. Newton and J. B. Keller. Stability of periodic plane waves. *SIAM J. Appl. Math.*, 47:959–964, 1987.

[24] B. S. Ng and W. H. Reid. An initial value method for eigenvalue problems using compound matrices. *J. Comp. Phys.*, 30:125–136, 1979.

[25] R. L. Pego. Compactness in L^2 and the Fourier transform. *Proc. Amer. Math. Soc.*, 95:252–254, 1985.

[26] R. L. Pego and M. I. Weinstein. Eigenvalues, and instabilities of solitary waves. *Phil. Trans. Roy. Soc. London A*, 340:47–94, 1992.

[27] M. Quiroga-Teixeiro and H. Michinel. Stable azimuthal stationary state in quintic nonlinear media. *J. Opt. Soc. Am. B*, 14(8):2004–2009, 1997.

[28] J. Shatah and W. Strauss. Instability of nonlinear bound states. *Comm. Math. Phys.*, 100:173–190, 1985.

[29] A. Soffer and M. I. Weinstein. Resonances, radiation damping and instability in Hamiltonian nonlinear wave equations. *Invent. Math.*, 136:9–74, 1999.

[30] I. Towers, A. Buryak, R. Sammut, and B. A. Malomed. Stable localized vortex solitons. *Phys. Rev. E*, 63:055601(R), 2001.

[31] I. Towers, A. V. Buryak, R. A. Sammut, B. A. Malomed, L.-C. Crasovan, and D. Mihalache. Stability of spinning ring solitons of the cubic-quintic nonlinear Schrödinger equation. *Phys. Lett. A*, 288:292–298, 2001.

[32] M. I. Weinstein. Nonlinear Schrödinger equations and sharp interpolation estimates. *Comm. Math. Phys.*, 87:567–576, 1983.

[33] M. I. Weinstein. Modulational stability of ground states of nonlinear Schrödinger equations. *SIAM J. Math. Anal.*, 16:472–491, 1985.

[34] M. I. Weinstein. Lyapunov stability of ground states of nonlinear dispersive evolution equations. *Comm. Pure Appl. Math.*, 39:51–68, 1986.

[35] E. M. Wright, B. L. Lawrence, W. Torruellas, and G. Stegeman. Stable self-trapping and ring formation in polydiacetylene *para*-toluene sulfonate. *Opt. Lett.*, 20(24):2481–2483, 1995.

Figure 1: Equal area construction for kink frequency

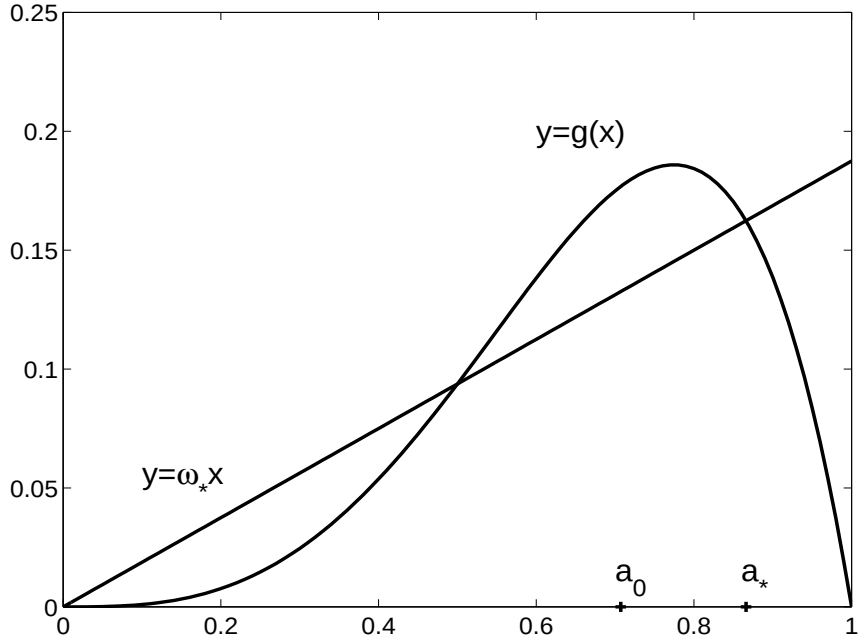

Figure 2: Potentials for cubic and cubic-quintic nonlinearities

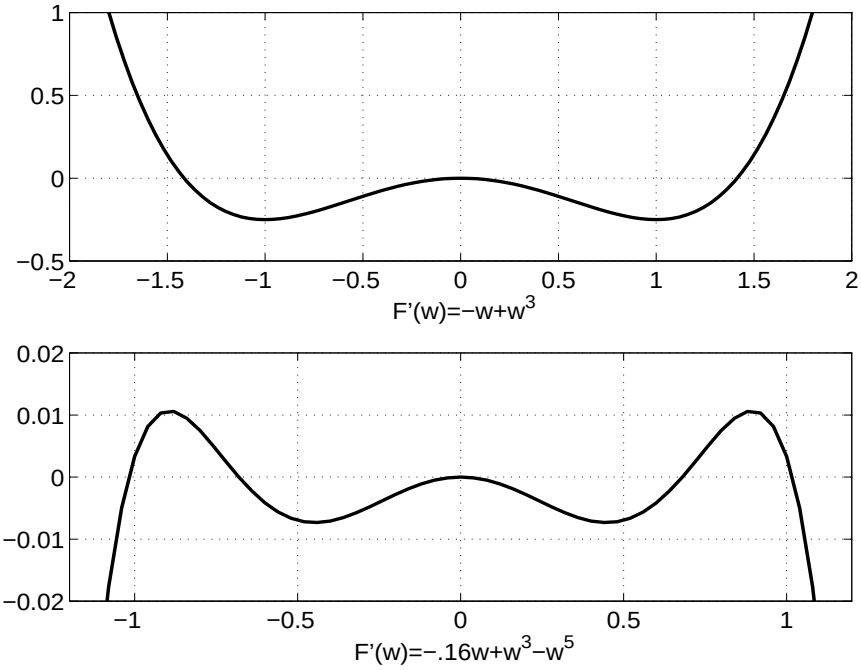

Figure 3: Nodeless profiles for cubic with varying spin m

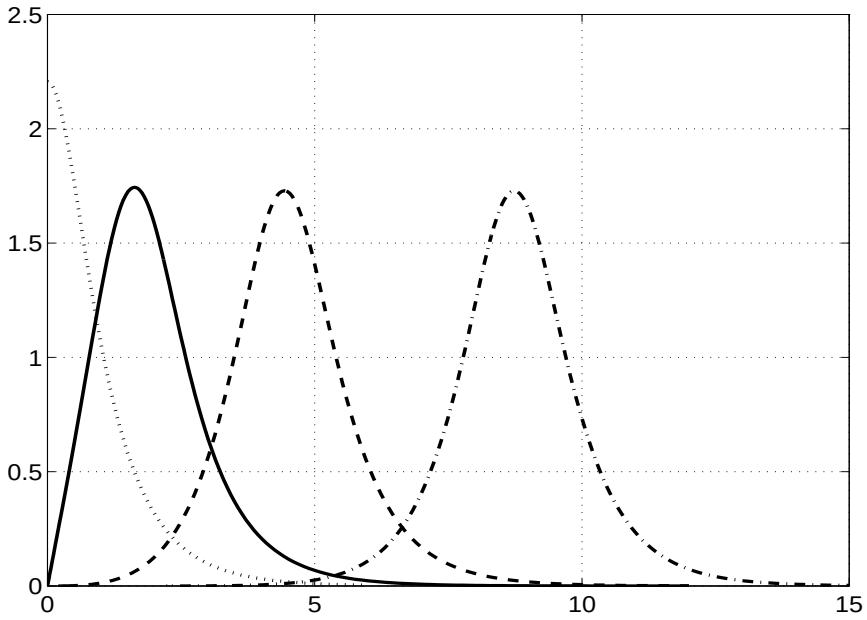

Figure 4: Nodeless profiles for cubic-quintic with $\omega = 0.18$, varying spin m

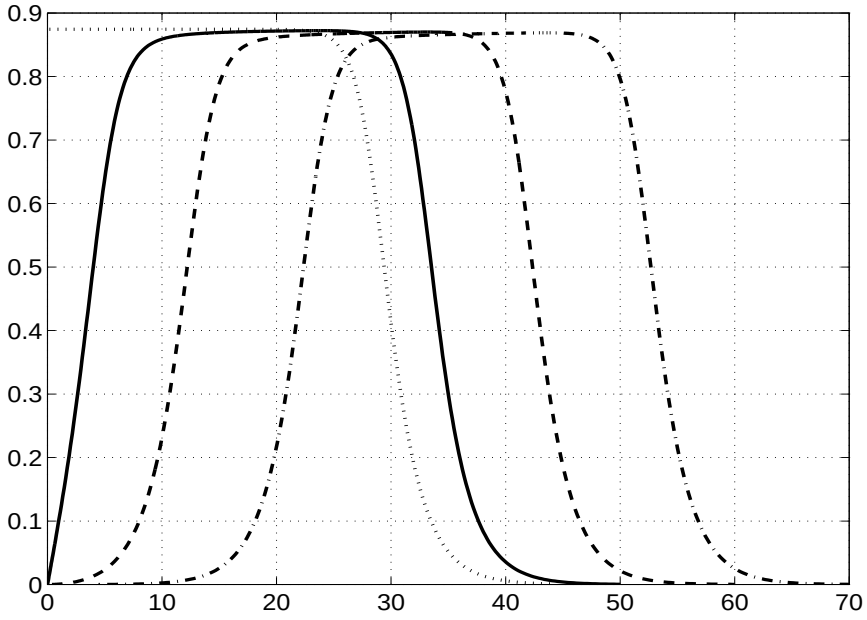

Figure 5: Nodeless profiles with $m = 1$ for cubic-quintic, varying ω

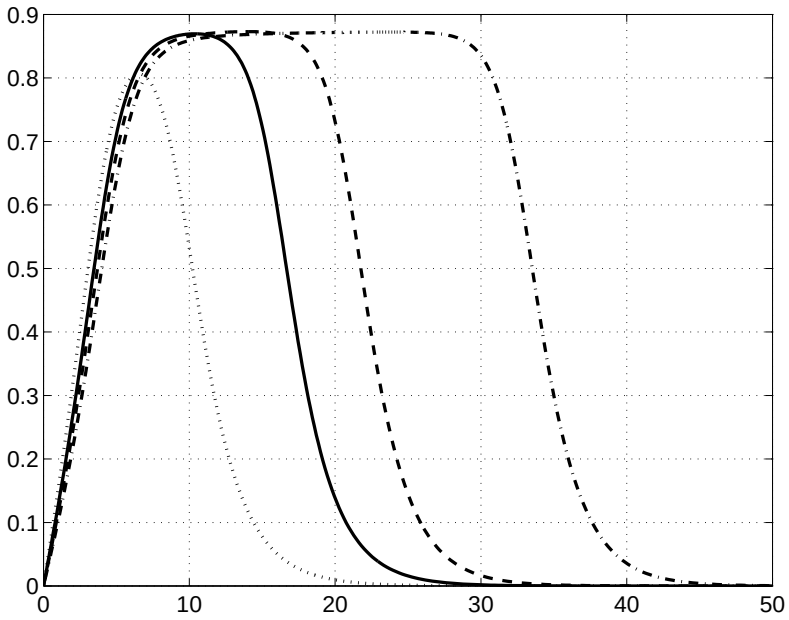

Figure 6: Nodeless profiles with $m = 3$ for cubic-quintic, varying ω

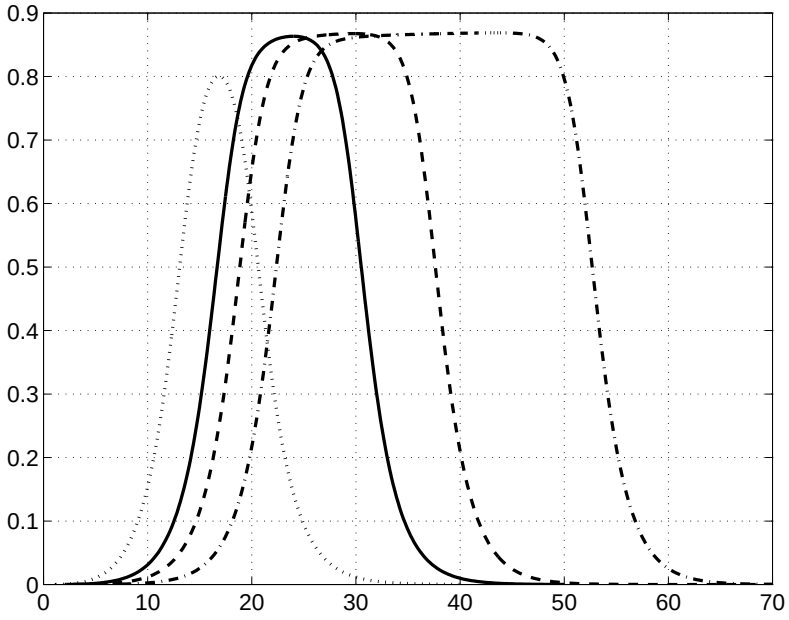

Figure 7: Schematic of contour used for counting eigenvalues

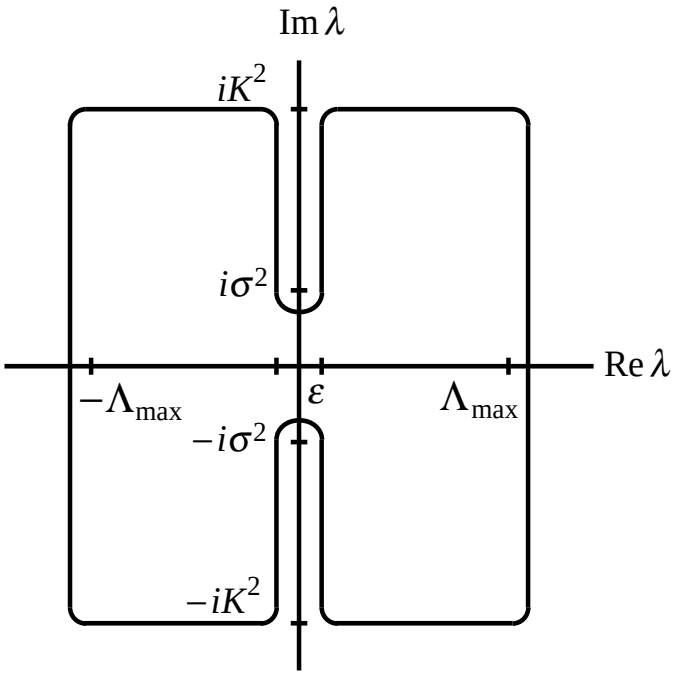

Figure 8: $E_2(it)$ *vs.* t near instability transition for $m = 1$, $\omega = .154$ and .145

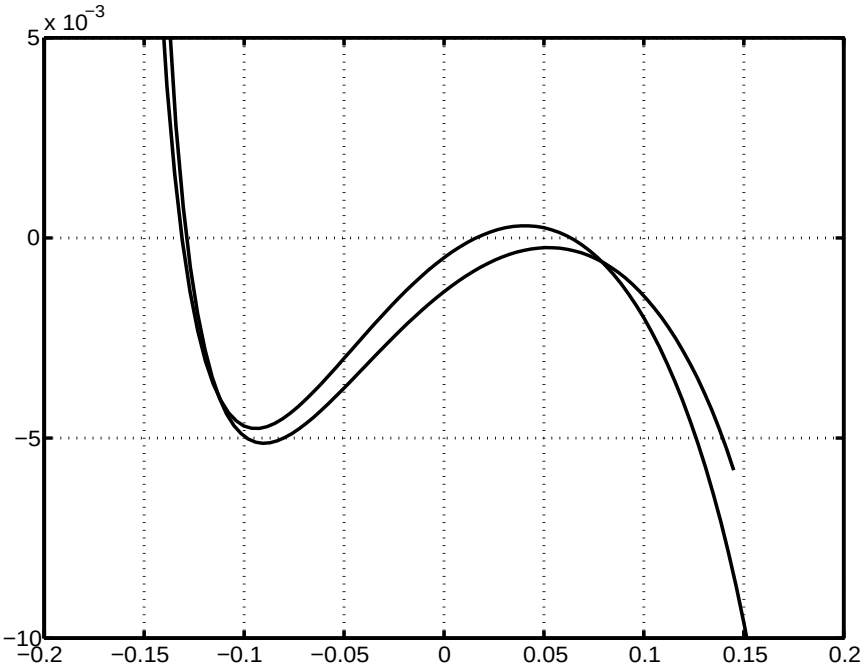

Figure 9: Profiles at stability transition for $m = 1, 2, 3, 4, 5$

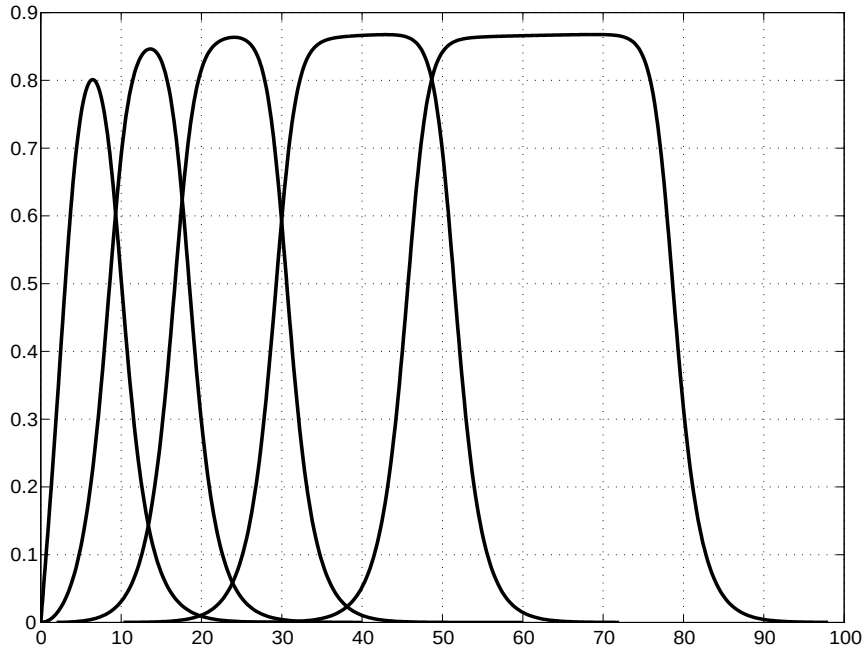

Figure 10: Stability transition: $\log_{10}(\omega_* - \omega)$ *vs.* $\log_{10} m$ for cubic-quintic case